

Project acronym:	Geo-Drill		
Project title:	Development of novel and cost-effective drilling technology for geothermal Systems		
Activity:	LCE-07-17-Renewables		
Call:	H2020-LC-SC3-2018-RES-TwoStages		
Funding Scheme:	RIA	Grant Agreement No:	815319
WP 2	Development of Materials and Coatings		

D2.9 Report on the development of materials and coatings

Due date:	30/09/2020 (M18)		
Actual Submission Date:	26/05/2021		
Lead Beneficiary:	TWI, GRA, CEA, PVI		
Main authors/contributors:	TWI, GRA, CEA, PVI		
Dissemination Level¹:	PU		
Nature:	REPORT		
Status of this version:		Draft under Development	
		For Review .by Coordinator	
	X	Submitted	
Version:	1.0		
Abstract	The deliverable reports the development of materials and coatings for Geo-Drill components		

REVISION HISTORY

Version	Date	Main Authors/Contributors	Description of changes
V1			

¹ Dissemination level security:

PU – Public (e.g. on website, for publication etc.) / **PP** – Restricted to other programme participants (incl. Commission services) /

RE – Restricted to a group specified by the consortium (incl. Commission services) / **CO** – confidential, only for members of the consortium (incl. Commission services)

GEODRILL



This project has received funding from the *European Union's Horizon 2020 research and innovation programme* under grant agreement No 815319.



This project has received funding from the European Union's Horizon 2020 program Grant Agreement No 815319. This publication reflects the views only of the author(s), and the Commission cannot be held responsible for any use which may be made of the information contained therein.

Copyright © 2019-2023, Geo-Drill Consortium

This document and its contents remain the property of the beneficiaries of the Geo-Drill Consortium and may not be distributed or reproduced without the express written approval of the Geo-Drill Coordinator, TWI Ltd. (www.twi-global.com)

THIS DOCUMENT IS PROVIDED BY THE COPYRIGHT HOLDERS AND CONTRIBUTORS "AS IS" AND ANY EXPRESS OR IMPLIED WARRANTIES, INCLUDING, BUT NOT LIMITED TO, THE IMPLIED WARRANTIES OF MERCHANTABILITY AND FITNESS FOR A PARTICULAR PURPOSE ARE DISCLAIMED. IN NO EVENT SHALL THE COPYRIGHT OWNER OR CONTRIBUTORS BE LIABLE FOR ANY DIRECT, INDIRECT, INCIDENTAL, SPECIAL, EXEMPLARY, OR CONSEQUENTIAL DAMAGES (INCLUDING, BUT NOT LIMITED TO, PROCUREMENT OF SUBSTITUTE GOODS OR SERVICES; LOSS OF USE, DATA, OR PROFITS; OR BUSINESS INTERRUPTION) HOWEVER CAUSED AND ON ANY THEORY OF LIABILITY, WHETHER IN CONTRACT, STRICT LIABILITY, OR TORT (INCLUDING NEGLIGENCE OR OTHERWISE) ARISING IN ANY WAY OUT OF THE USE OF THIS DOCUMENT, EVEN IF ADVISED OF THE POSSIBILITY OF SUCH DAMAGE.

Date: 25 January 2023

Summary

This deliverable describes work that was performed to develop materials and coatings using a wide range of technologies in Work Package (WP) 2, including:

- **GO-enhanced tungsten carbide material development for drill bit tooth and fluidic oscillator**
Led by GRA, a blending process of WC-Co/GO (rGO) was developed to obtain a good dispersion of GO in WC powder. Both pure WC-Co and WC-Co/GO bulk materials were prepared through sintering and are due to be tested in WP3.
- **Development of GO based coating**
Led by GRA, this includes preparing coatings using graphene oxide (GO) for both hammer parts and sensors. To develop coating for hammer parts, the mixture of GO with the Xylan was successful and the processability of the mixtures is a key parameter. Samples at four different GO concentrations were prepared and will be analysed in WP3. Preliminary testing carried out by University of Iceland indicated that of the concentrations tested, the best performance came from the extra low wt% GO in the Xylan samples. For the sensors, powder mixtures of PTFE and GO were developed to introduce in PVI's polymeric matrix. After parametrisation and preparation of the mixtures, PVI prepared the inks, and the screen-printed samples were sent to WP3 for further characterisation and down-selection of the best candidate.
- **Development of coating for drill bit tooth, fluidic oscillator, and stabiliser;**
Led by TWI, coating systems including tungsten carbide (WC) coatings, chromium carbide (CrC) coatings, self-fluxing alloy (NiCrFeSiB) coatings, and nano-crystalline/amorphous coatings, were developed using high-velocity oxygen fuel (HVOF) process. Down-selection was determined by comparing surface roughness, microstructure, deposition efficiency, porosity, hardness and adhesion strength of the coatings. The selected coatings have surface roughness ranges from 3.5 to 8.5 μm , porosity ranges from 0.9 to 3.6%, and hardness ranges from 661 to 1218HV_{0.3}.
- **Development of HIP bonding process for drill bit tooth;**
Led by CEA, a manufacturing route for the drill bit using HIP as a technical solution was investigated to bond the WC-Co inserts onto the drill bit. Two materials were selected, the cemented tungsten carbide for the hard inserts and the low alloy steel for the head and shank of the drill bit. Direct bonding of WC-Co tooth to 4330V steel at 1160°C/102MPa/3h led to a weak interface. The use of a selected interlayer enabled fabrication of a crack free WC-Co/4330V joint after HIPing. However, cracking of WC-Co tooth was noticed after post-treatment. This was attributed to martensitic transition during quenching and can be overcome by changing the heat treatment specification. It is proposed to stop quenching at a temperature above the martensite transition and then to cool slowly under calm air before doing final tempering heat treatment.
- **Development of diffusion bonding process for tool joint and drill stabilizer;**
Led by CEA, the bonding of two high strength alloys (FeNiCo and NiCrMo) to 4140 steel were studied using HIP. HIP bonding was done by applying anti-diffusion foils and results indicate that a 1mm thick interlayer avoids carburization of both alloys. Post HIP heat treatments were performed on the manufactured joints to harden the 4140 to the required hardness. Tensile tests showed that the bonded joints have much lower impact toughness compared with 4140. It is proposed that wear resistance of tool joint can be improved by bonding a 5mm thick FeNiCo ring on the shoulder at 1100°C/102MPa/3h, following post heat treatments. A similar manufacturing process can be used for fabrication of stabilizer.

D2.9 Report on the development of materials and coatingsVersion:

Date: 25 January 2023

- **Development and synthesis of sensor materials;**
Led by PVI, nano-particle inks were being studied with tailored resistivity for use in strain gauge, temperature and encoder sensors above 250°C. Inks for temperature sensors to operate between -40°C and 250°C were also under development. Materials have been identified for a piezoelectric energy conversion device and for a printed triaxial accelerometer for the down-the-hole environment.
- **Development of Electroless plating for PTFE based composite coatings ;**
Led by TWI, an electroless nickel-phosphorus plating process for PTFE based composite coatings on low alloy steel substrate material has been developed. Initial trials were performed on mild steel substrates for developing the procedure and to produce high quality duplex coatings with excellent adhesion to the substrate. Bath compositions were developed for the production of low phosphorus (P) and high P coatings. Additionally, heat treatments were also performed to alter the microstructure by generating crystalline phases to improve the coating's mechanical and tribological properties. The effect of heat treatments on the performance of the coatings was compared with those in the as-plated condition by conducting microstructural characterisation, cross-cut testing, Knoop hardness measurements, and sliding wear tests in dry and wet conditions. It was observed that the specimens having high P undercoat and low P+PTFE topcoat, heat-treated at 300°C for 2 hours had better mechanical and tribological properties compared with the rest of the coatings. The down-selected coating was produced on the low alloy steel specimens for WP3 for further testing.
- **Development of HEA and cermet coating.**
Led by TWI, coating systems including high entropy alloy (HEA), WC-Ni and WC-CrC-Ni coatings were developed using high-velocity oxygen fuel (HVOF) process. Down-selection was determined by comparing surface roughness, microstructure, deposition efficiency, porosity, hardness and adhesion strength of the coatings. The optimised coatings have surface roughness ranges from 3.9 to 6.6 µm, porosity ranges from 1.6 to 2.0%, and hardness ranges from 558 to 1077 HV_{0.3}.

Objectives Met

The work described contributes to the following WP2 objective:

- To synthesise materials, coatings and develop coating technique for Geo-Drill components:
 - a) Drill bit tooth
 - b) Fluidic hammer
 - c) Sensors
 - d) Drill stabiliser
 - e) Tool joint

D2.9 Report on the development of materials and coatingsVersion:

Date: 25 January 2023

CONTENTS

SUMMARY.....	4
OBJECTIVES MET.....	5
CONTENTS.....	6
1. OVERVIEW.....	7
2. TASKS.....	7
TASK 2.1: GO-ENHANCED TUNGSTEN CARBIDE MATERIAL DEVELOPMENT FOR DRILL BIT TOOTH AND FLUIDIC OSCILLATOR	7
TASK 2.2: DEVELOPMENT OF GO BASED COATING.....	12
TASK 2.3: DEVELOPMENT OF COATING FOR DRILL BIT TOOTH, FLUIDIC OSCILLATOR, AND STABILISER.....	16
TASK 2.4: DEVELOPMENT OF HIP BONDING PROCESS FOR DRILL BIT TOOTH	16
TASK 2.5: DEVELOPMENT OF DIFFUSION BONDING PROCESS FOR TOOL JOINT AND DRILL STABILISER.....	33
TASK 2.6: DEVELOPMENT AND SYNTHESIS OF SENSOR MATERIALS.....	51
TASK 2.7: DEVELOPMENT OF ELECTROLESS (EL) PLATING FOR SYNTHESIS OF PTFE BASED COMPOSITE COATING.....	53
TASK 2.8: DEVELOPMENT OF HEA AND CERMET COATING	63
3. CONCLUSIONS.....	63
REFERENCES.....	64

Date: 25 January 2023

1. OVERVIEW

This report covers a range of activities for the development of materials and coatings for Geo-Drill components. This includes:

- Development of process for mixing WC-Co and graphene oxide (GO) materials and sinterization;
- Introduction of GO materials into state-of-the-art coatings. This include preparing inks with PTFE and GO for both hammer parts and sensors;
- Development of HVOF coatings, including tungsten carbide (WC) coatings, chromium carbide (CrC) coatings, self-fluxing alloy (NiCrFeSiB) coatings, and nano-crystalline/amorphous coatings;
- Development of HIP bonding process for drill bit tooth;
- Development of diffusion bonding process for tool joint and drill stabilizer;
- Development and synthesis of sensor materials;
- Development of Electroless plating for PTFE based composite coatings;
- Development of High Entropy Alloy (HEA) and cermet coatings.

2. TASKS

Task 2.1: GO-enhanced tungsten carbide material development for drill bit tooth and fluidic oscillator

Within Task 2.1 Graphenea has explored the viability of mixing tungsten carbide (WC) powder with graphene oxide (GO) materials in order to improve the tribological properties of the WC. A ball milling process has been developed and bulk pieces have been prepared to be tested in WP3.

By the oxidation of graphite using strong oxidising agents, oxygenated functionalities are introduced in the graphite structure making the material hydrophilic. On the other hand, the increase of the interlayer distance makes the interaction between flakes weaker. These properties enable the graphite oxide to be exfoliated in water using sonication, ultimately producing graphene with a single layer or relatively few layers, known as graphene oxide (GO). This is illustrated in Figure 1.

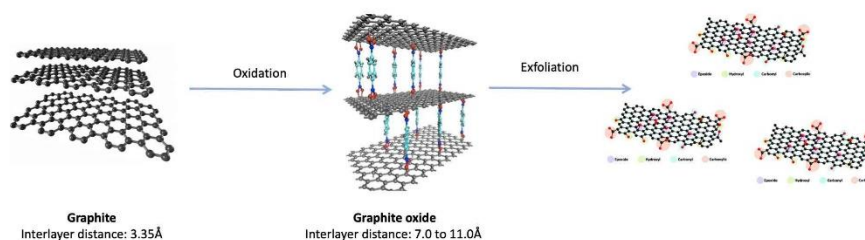


Figure 1: Graphene oxide formation

The large number of oxygen moieties of the GO make it compatible with a large number of matrices and very versatile in terms of chemical modification. Oxygen functional groups can be removed and the sp^2 structure recovered to obtain reduced graphene oxide (rGO) or the functionalities can be tuned to make the material more compatible with the matrix. Due to its high surface area, a low quantity of filler is usually needed to improve properties.

Graphene oxide was produced using a modified Hummers method (GRAPHENEA's methodology: patent EP15382123 2015): graphite powder was dispersed in H_2SO_4 and cooled down. Then $KMnO_4$ was added to the mixture. After stirring for 1h the mixture was heated up to $30^\circ C$ and kept at this

D2.9 Report on the development of materials and coatingsVersion:

Date:

25 January 2023

temperature for 4h. The mixture was cooled down and distilled water was slowly added. The solution was stirred 30 min and then distilled water was again added. Finally, H₂O₂ was added and the colour become yellow. This dispersion was purified by cleaning with distilled water and GO slurry (water dispersion) was obtained. With this methodology a GO with 43-45% of oxygen is obtained. Figure 2 shows the evolution of X-ray diffraction (XRD) peaks when graphite is reacted, and GO is produced. It can be observed how the 2θ peak of graphite (~26°) decreases to lower angles (~10°), indicating an increase in the interplanar distance. Moreover, when GO is reduced a broad peak can be observed (~24°) at similar angles to the graphite though with a more amorphous structure.

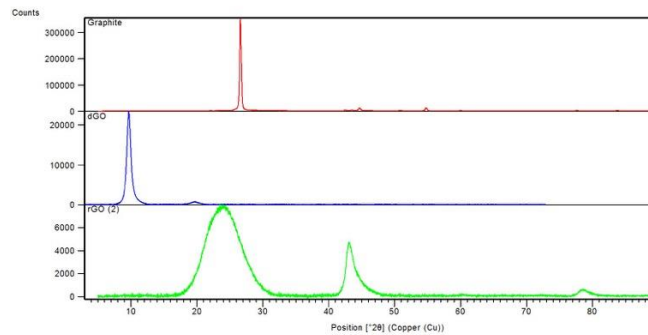


Figure 2: XRD spectra of the different products: Red – graphite; Blue – graphene oxide; Green – reduced graphene oxide

The synthesis of GO not only involves the reaction, but also purification steps to eliminate different salts and impurities that remain after the reaction, and subsequent dispersion steps. Therefore, the fabrication of water dispersed graphene oxide monolayers implies different steps: 1) Production of graphite oxide from graphite (Hummer's modified method); 2) Purification of graphite oxide; 3) Dispersion/exfoliation to obtain graphene oxide monolayer (Figure 3). If powder is needed an atomisation (spray dry) process is carried out.

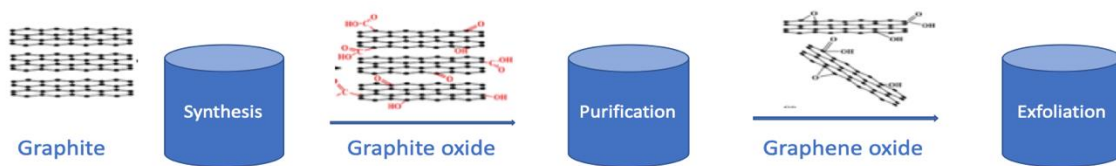


Figure 3: Synthesis, purification and exfoliation of the graphene oxide

Graphenea has a range of different materials in its portfolio (Figure 4). Starting from the GO slurry (2.5 wt%), GO dispersions of different concentration can be prepared by stirring and sonicating. It can be dried (in a spray dryer) to obtain a fine powder, part of the oxygen content can be removed recovering the sp² structure to get a reduced graphene oxide (rGO) fine powder and it can be also aminated (all the powders are fabricated by processing dispersions in a spray dryer). During development of the composition and the fabrication process a large quantity of materials of different nature was utilised. Graphenea has a pilot production plant in which GO is fabricated in kg batches. This GO is synthesised in a pilot reactor and purified in two different centrifuge systems to obtain GO in slurry format. All materials are reproducible and exhaustive quality control is performed to ensure the quality: TGA (thermogravimetric analysis), XRD, elemental analysis and viscosity (if necessary).

D2.9 Report on the development of materials and coatingsVersion:

Date: 25 January 2023

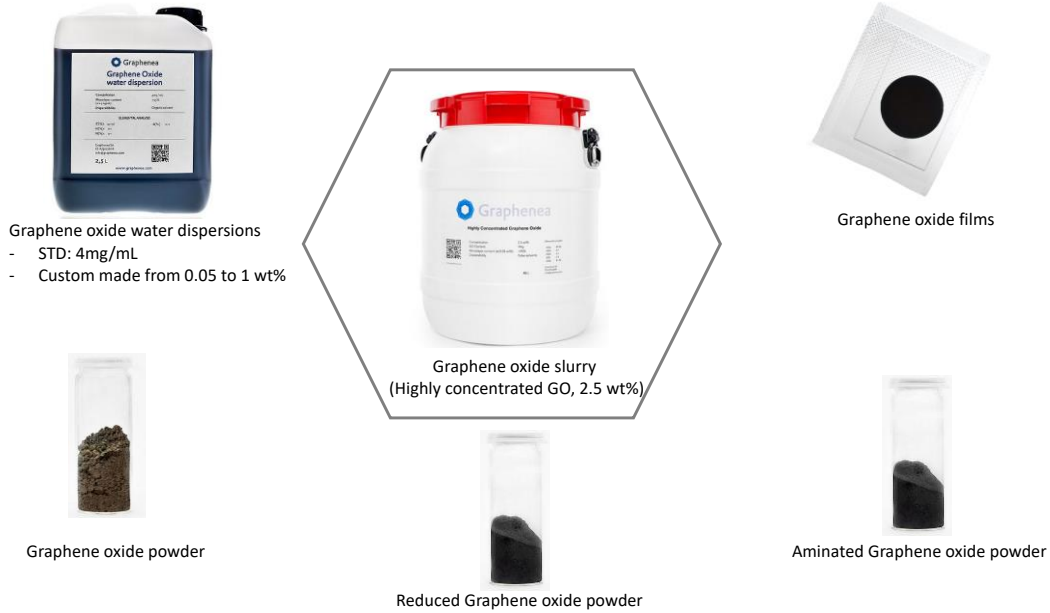


Figure 4: Graphenea’s product portfolio

WC/GO composites

Powder mixing

In the literature only one reference regarding WC-Co/GO mixtures [1] was found and in this study the final objective was not to fabricate solid bulk pieces; the mixture was spray coated. For this reason, in order to have an idea of the mixing conditions, articles in which the WC was mixed with other nanoparticles were researched and Ref [2] was found.

CEA carried out an investigation to understand the effect of the addition of carbon to WC materials, as it can influence the properties of the final product. Also, within the consortium the WC material to be used was decided.

After making the decision of the percentage of C needed and taking into account the information found in the literature, blending between the GO powder/WC-Co mixture was carried out in an alcohol media to avoid oxidation. The ball mill system’s velocity and time were adjusted to identify a satisfactory process.

The best conditions were chosen after analysing the materials in the SEM. In the following image a comparison of the raw GO powder (Figure 5), the raw WC-Co and the mixture is presented. The GO forms a thin film that wraps the WC particles.

D2.9 Report on the development of materials and coatingsVersion:

Date: 25 January 2023

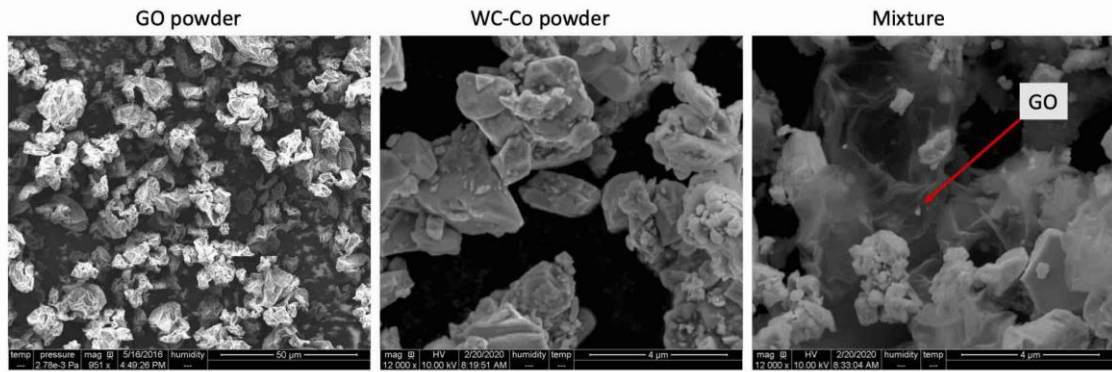


Figure 5: SEM analysis of the materials

Sintering

The as-fabricated powders need to be sintered in a shape that can be tested in WP3. Within the consortium no partner had the capabilities to do the sintering so a French Company was found that could carry this out using their established conditions for WC-Co. In Figure 6 the manufactured pieces are shown. It is clearly observed, with no further analysis, that the GO has a negative impact on the integrity of the sintered pieces but as will be shown in deliverable 3.1 the tribological properties were improved.



Figure 6: GO/WC fabricated pieces (left, neat WC-Co, right WC-Co + GO)

Use of reduced graphene oxide

In order to improve the integrity of the samples, it was decided to try reduced graphene oxide (rGO). This material is chemically reduced and part of the sp^2 hybridisation is recovered at the same time that the oxygen content decreases. Consequently, the material is more thermally stable (Figure 7).

D2.9 Report on the development of materials and coatingsVersion:

Date:

25 January 2023

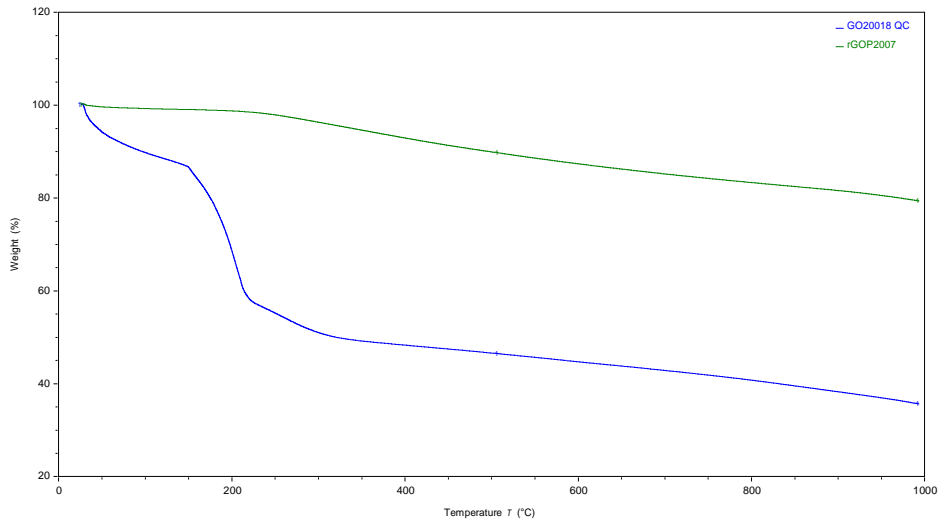


Figure 7: comparative TGA og GO and rGO

The development process was similar to the one carried out for the GO. The SEM analysis of the materials is presented in Figure 8.

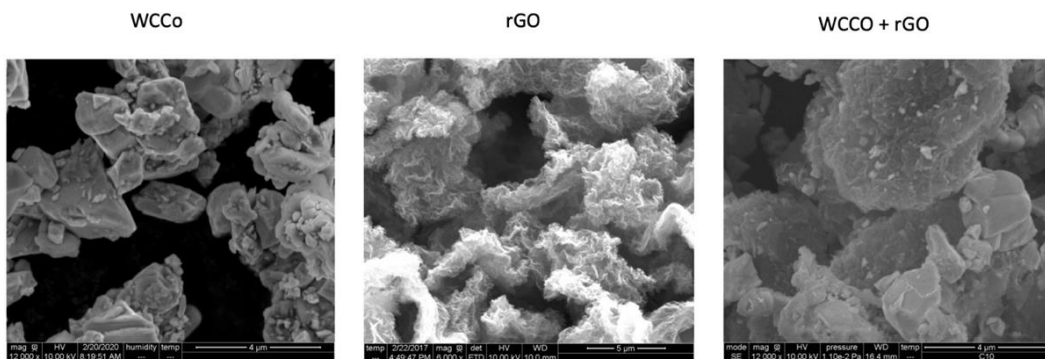


Figure 8: SEM analysis of the materials

The use of a more thermally stable material led to improved pieces that will also be tested in WP3 (Figure 9).



Figure 9: rGO/WC-Co pieces

Task 2.2: Development of GO based coating

GO- Based Hammer Coating Manufacture and Properties

After exploring different approaches, it was decided to work on the improvement of the properties of the commercially available coating, Xylan. Investigation of different mixing parameters was successfully carried out and a coating process was developed. Several samples with different GO content were prepared and substrates were sent to WP3 to be tested. Based on the preliminary results a preferred formulation was selected, and additional samples were prepared for further analysis in WP3.

One of the objectives of the Geo-Drill project is to improve the lifetime of the drilling components. The geothermal drilling environment is extremely challenging in terms of temperature, pressure, rock breaking etc. Components are subjected to wear, material fatigue, erosion and breakage. To improve wear and erosion resistance of these components graphene oxide (GO) based coatings were investigated.

As mentioned in Task 2.1, the oxygen functionalities present on graphene oxide make it compatible with a large range of polar matrices. As an example, in a previous work Graphenea demonstrated an improvement of 50% in the wear behaviour of Al_2O_3 by the addition of only 0.22 wt% GO [1].

Most of the research articles about PTFE/GO refer to membranes (desalination of water, LiS batteries etc) but there is not much information regarding composites. The following article was found in which the best results were obtained with the addition of 15 % volume of graphene oxide[3]. PTFE powder was used and dispersed in water and GO was added and sonicated. The mixture was spin-coated and after thermal treatment, the properties were tested. Wear rate was reduced from $5.6 \cdot 10^{-8}$ to $1.9 \cdot 10^{-9} \text{ mm}^3 \text{ N}^{-1} \text{ m}^{-1}$ and the coefficient of friction (COF) was reduced from 0.16 to 0.045.

A coating can be considered as an engineering material as it usually includes in its composition a lot of additives to make it stable and compatible with surfaces. Looking for special additives to be added in order to improve our coatings, commercial formulations were found. After contacting some companies, Graphenea had a meeting with Whitford. A PTFE based coating (Xylan) which is already used in the oil and gas industry was recommended.

The commercially available Xylan coating is a dark grey viscous liquid and therefore it is difficult to distinguish the graphene oxide materials inside the mixture. Taking into account the previous experience, this time it was decided to proceed with low concentrations. The dispersions seemed homogeneous and with no agglomerations. In the images from the optical microscope it was not possible to identify the graphene oxide. The viscosity of the mixtures affects the processability. To study the impact of the addition of GO materials on the processability, mixtures of GO powder and rGO powder containing three different concentrations were prepared. With both materials it was a limit in which the material was not processable but the addition of a small amount of water helped with the coating. The GO blends were more homogeneous and easier to process than the rGO ones.

In Table 1 a summary of the parameter development trials is presented.

D2.9 Report on the development of materials and coatingsVersion:

Date: 25 January 2023

Table 1: Parameter development

Matrix	Filler	Wt%	Mixing	Comment
Xylan	GO powder	low	High shear mixer	OK
Xylan	GO powder	low	High shear mixer 2xtime	OK
Xylan	GO powder	low	High shear mixer 3xtime	OK
Xylan	GO powder	medium	High shear mixer	High viscosity
Xylan	GO powder	high	High shear mixer	Paste
Xylan	GO powder +water	high	High shear mixer	Liquid
Xylan	GO slurry	low	High shear mixer	Liquid
Xylan	GO slurry	high	Not processable	Paste
Xylan	GO slurry + water	high	High shear mixer	Liquid
Xylan	GO powder	low	High shear mixer	OK
Xylan	GO powder + water	medium	High shear mixer	OK
Xylan	rGO powder	low	High shear mixer	OK
Xylan	rGO powder	medium	High shear mixer	High viscosity
Xylan	rGO powder	high	Not processable	Paste
Xylan	rGO powder + water	high	High shear mixer	Liquid

After obtaining the preferred parameters to produce the mixtures, the pieces to be tested in the WP3 were fabricated, coated and sent to WP3 to study (Table 2, Figure 10).

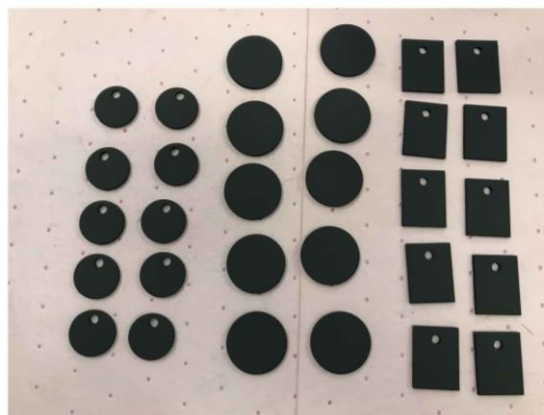


Figure 10: example of coated samples

D2.9 Report on the development of materials and coatingsVersion:

Date:

25 January 2023

Table 2: samples prepared

Substrate	Coating	Nº samples	Comments
Uol tribo-corrosion	Xylan	10	
	Xylan + extra low wt% GO	10	Totally covered
	Xylan + low wt% GO	10	
	Xylan + medium wt% GO	10	
	Xylan + high wt% GO	10	
	Xylan + low wt% GO	5	Totally covered
	Xylan + medium wt% GO	5	Totally covered
	Xylan + medium wt% GO	10	Totally covered
	Xylan + high wt% GO	5	Totally covered
Uol tribo-rotating	Xylan	10	
	Xylan + extra low wt% GO	10	
	Xylan + low wt% GO	10	
	Xylan + medium wt% GO	10	
	Xylan + medium wt% GO	10	
	Xylan + high wt% GO	10	
Uol tribo-reciprocating	Xylan	10	
	Xylan + extra low wt% GO	10	
	Xylan + low wt% GO	10	
	Xylan + medium wt% GO	10	
	Xylan + medium wt% GO	10	
	Xylan + high wt% GO	10	
Uol Cylindrical	Xylan	10	
	Xylan + medium wt% GO	10	
Uol Coupon	Xylan	10	
	Xylan + medium wt% GO	10	
	Xylan + low wt% GO	10	
	Xylan + extra low wt% GO	10	
Rina Ring on ring RT	Xylan	10	
Rina Ring on ring HT	Xylan	10	
Rina Sliding	Xylan	10	
Rina Tribo-corrosion	Xylan	10	
Rina Adhesion	Xylan	10	
Rina Tribo-corrosion	Xylan	5	
	Xylan + extra low wt% GO	5	
TWI	Xylan	8	
	Xylan + extra low wt% GO	8	
	TOTAL	341	

Date: 25 January 2023

GO based sensor coating manufacture and properties

Among the components that the Geo-Drill project seeks to protect, sensors are crucial, as their electronic parts need to be isolated from the extremely challenging drilling environment. In this sense, the proposed strategy was to cover the sensors with a final coating consisting of a mix of GO-based material with PTFE combined with a high temperature (> 280°C) polymer matrix incorporated into the formulation to make it suitable for screen printing and thermal set curing.

Two different mixtures in powder format were selected (Figure 11). Manual blending in a ceramic mortar was initially carried out but the samples were not homogeneous. With a small ball milling system, the results were improved. Powder quantities, velocities, number of balls and time were varied, and the preferred parameters were selected.

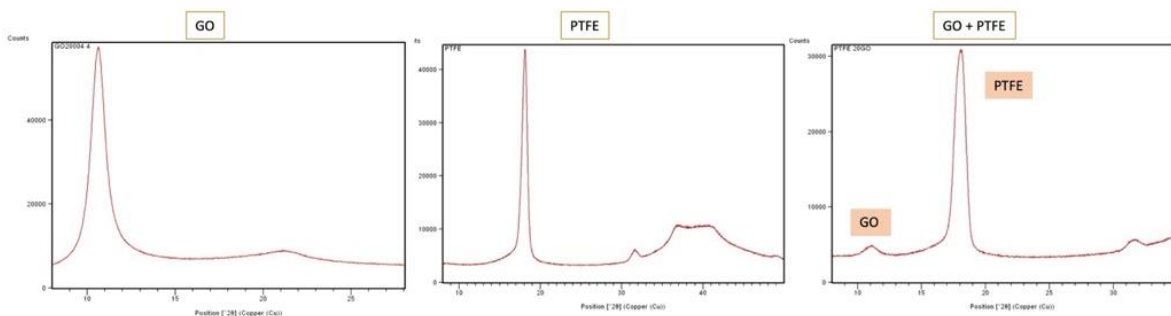


Figure 11: XRD characterisation of the powders

After process validation and material characterisation the material listed in Table 3 was fabricated.

Table 3: Material sent to PVI

Mixture	PTFE powder	GO powder	Total amount
1	100%	0%	125g
2	100-x %	x%	125g
3	100-2x %	2x%	125g
4	0%	100%	125g

PVI prepared inks with these powders (Figure 12). The inks need to be suitable for screen printing. When only GO was introduced in their formulation, the rheology was not adequate. This happens due to the high aspect ratio of the GO that has a direct influence in the viscosity of the mixture.

Date:

25 January 2023

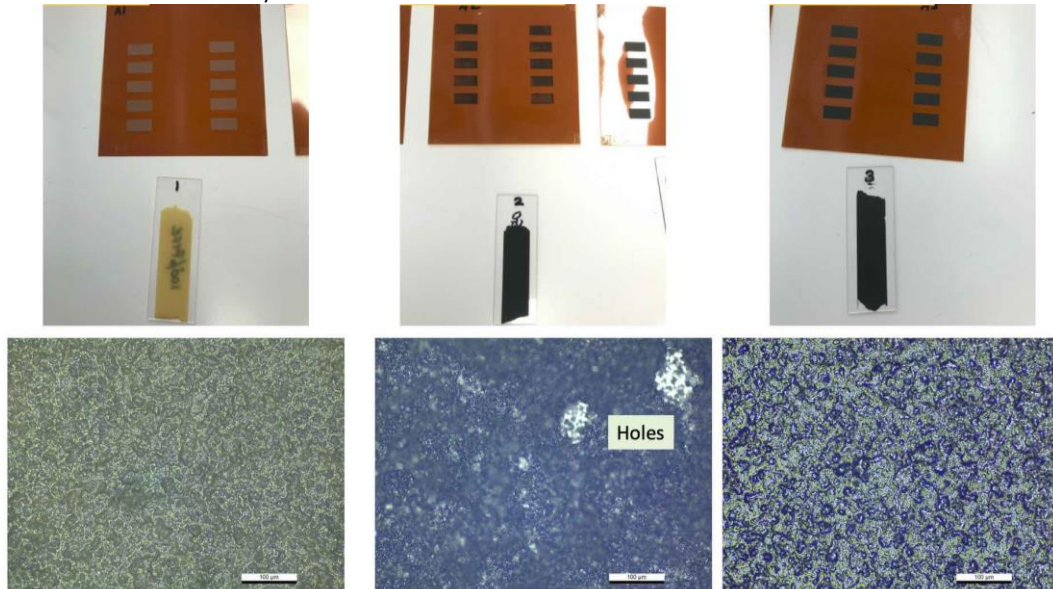


Figure 12: Screen printed samples and the optical microscope images

Task 2.3: Development of coating for drill bit tooth, fluidic oscillator, and stabiliser

Please refer to D2.4 of Geo-Drill submitted deliverables.

Task 2.4: Development of HIP bonding process for drill bit tooth

Introduction

In the geothermal environment, wellbores are drilled by simultaneous percussive and rotation movements of the bits driven by an air or a water hammer. To withstand the mechanical stress and the wear during drilling operations, drill bits are manufactured with low-alloyed steel, heat treated to reach the required hardness and their heads are equipped with very hard WC-Co inserts (WC-Co teeth).

Several techniques are used to attach or join the WC-Co inserts onto the drill bit head depending on the operating constraints. For low temperature applications (up to 200°C), press fit parts can be used. For higher temperatures, brazing is preferred but the reliability of this solution depends on several parameters such as the choice of the brazing filler alloy to perfectly wet the steel and the WC-Co and the final thickness of the brazing filler alloy to limit the residual stress inside the assembly. It also depends on the ability of the WC-Co inserts to support a quench if the brazing is done at high temperature to finally harden the steel to the required hardness. To avoid this last difficulty, brazing can be done on hardened steel if the brazing operation is done quickly at a moderate temperature.

In the GEODRILL project, where deep geothermal drilling is considered and temperatures as high as 250°C are expected, we investigate the possibility to anchor the WC-Co inserts to a low alloy steel by HIP. This technique enables solid-state diffusion bonding by the combined and simultaneous application of a high temperature and a high-pressure plateau for several hours. As this technique enables joining the base materials without a filler alloy, it is well adapted for high temperature applications. In addition, the HIP assembly method can be used for parts that have a complex shape to improve their mechanical anchoring as it is the case for the hard inserts onto the drill bit head.

D2.9 Report on the development of materials and coatingsVersion:

Date: 25 January 2023

To perform the necessary experimentations to find a route to manufacture the drill bit by HIP, we first selected the materials to join i.e. the WC-Co inserts and the low-alloyed steel. Then we proposed a new design for the hard inserts to favour their anchoring inside the steel before doing the HIP experiments and the post heat treatments to harden the steel to the required hardness. The results of our numerous experimentations are presented in this report and we conclude with a manufacturing route to fabricate drill bit prototype by HIP.

Selection of the materials to develop the HIP process and design of the hard inserts

WC-Co grade

The mechanical properties and the wear resistance of the WC-Co inserts depend on the WC grain size and on the Co content [4, 5]. Manufactured classically by powder metallurgy, the mechanical properties of WC-Co are also very sensitive to the characteristics of the blended powders (WC, Co and other added powders like carbon) and to the densification parameters. Imperfect densification parameters can lead to residual porosities inside the WC-Co inserts and to a loss of mechanical strength.

For percussive mining tools, a good compromise between fracture toughness and wear resistance is obtained with coarse or ultra-coarse WC grains and a Co content between 6 and 15 Wt. %. (Figure 13). To perform the work in Task 2.4, we have selected a grade with coarse WC grains and a Co content equal to 15Wt. %. The B40 grade from Element Six verify these specifications as it is shown in Figure 14. The teeth ordered to perform our study are made with this grade.

Steel grade

Very little information regarding steel grades to manufacture drill bits has been found in the literature (publications, patents). Steel manufacturers have proposed some grades (AISI 4330V or AISI 4337 (34CrNiMo6)). and we purchased one AISI 4330V bar manufactured by Carpenter. This bar was delivered in normalized and tempered condition with a Brinell hardness equal to 261HV30 and an ASTM grain size equal to 8. Table 4 gives the chemical composition of the steel bar, which conforms with the standard.

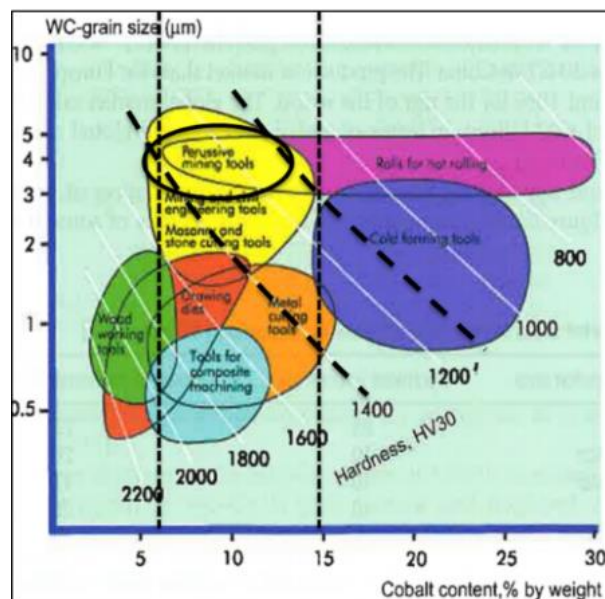


Figure 13: application range of straight cemented carbides grades (Sandvik Hardmaterials)[5]

Date: 25 January 2023

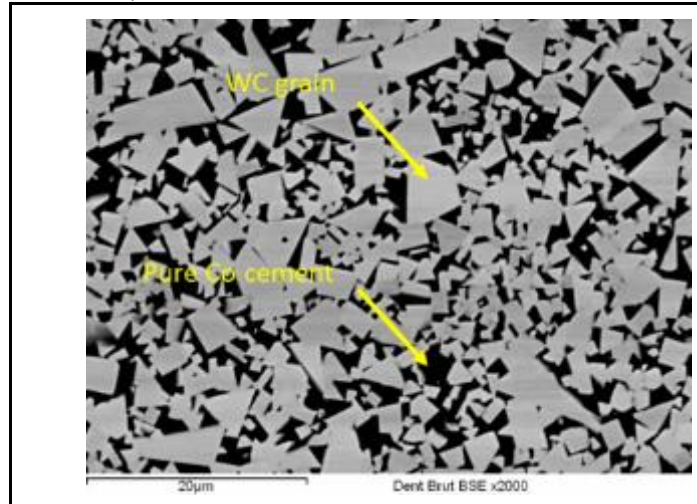


Figure 14: B40 grade from Element Six.

Table 4: chemical composition of the 4330V bar purchased from Carpenter.

4330V Grade	Chemical composition (wt.%)								
	C	Mn	Mo	Si	S	P	Cr	Ni	V
Chemical standard	0.30-0.34	0.75-1.00	0.40-0.50	0.15-0.35	0,035mx	0,035mx	0.75-1.00	1.65-2.00	0.05-0.10
As received	0.30-0.32	0.91-0.94	0.47	0.31-0.32	0.001	0.004	0.83	1.82	0.08

Design of the hard teeth

The shape of the WC-Co teeth was designed to favour their anchoring inside the steel drill bit (Figure 15). A conical shape was chosen. This shape is different from the traditional straight button shape found in all the commercial catalogues. Forty-eight B40 grade teeth were manufactured by Element Six. All of them were made by sintering before a final HIP consolidation cycle to close the residual porosities. High of them were polished to investigate the influence of the mean surface roughness of the teeth on the HIP joining process. In the as received state, the mean Vickers hardness of the material is equal to 1095HV30. A size control of some teeth taken randomly from the 40 teeth ordered shows that the teeth conform to the manufacturing drawing with dimensions in the range of the required tolerances ($\pm 0.25\text{mm}$).

Date: 25 January 2023

HIP cycle and post HIP heat treatments

The same HIP cycle was used to evaluate the fabrication of the drill bit with the two designs shown in Figure 16. It comprises a high temperature and a high-pressure of 1160°C and 102MPa for three hours. These parameters are commonly used in industry to heat treat cast alloy steels in large HIP vessels.

As the cooling rate in most HIP vessels is low (about 5°C/min), post heat treatments are done to give the required steel hardness. To reach a high hardness to support the shock of the hammer, the HIPed mock-ups were subjected to an austenitization heat treatment at 870°C for one hour, a quench and a tempering heat treatment done twice for two hours at the same temperature (as recommended by the 4330V steel manufacturers). The best tempering temperature to reach the required hardness has been determined experimentally by measuring the hardness of thick HIPed and quenched 4330V steel slices tempered twice at different temperatures for two hours. According to our measurements, a tempering temperature between 300°C and 420°C was chosen.

Mechanical properties of the WC-Co tooth, 4330V and 4330V/4330V joint after post HIP heat treatments

After HIP, Vickers hardness measurements are done on a WC-Co tooth to quantify the influence of the 1160°C/102MPa/3h HIP cycle on its mechanical properties. Measurements are made from the top surface of the tooth to its centre. A mean hardness of about 1150HV0.1 is measured, which is very close to the hardness value of the as received material. Therefore, HIP cycle has no influence on the hardness of the WC-Co cermet. This result was expected because the sintering process of the cermet is done at a much higher temperature than the HIP temperature.

The mechanical properties of the 4330V/4330V joint and the bulk 4330V steel are evaluated after post HIP heat treatments by performing tensile tests and KV impact toughness tests at 20°C and 250°C (250°C is the expected maximal operating temperature of the bit). These values are important to verify if the second assembly design can be used to manufacture the drill bit. The tensile specimens are machined from a mock-up constituted by two round pieces (Figure 17) HIPed together at 1160°C/102MPa/3h and then post heat-treated to temper the steel to the required hardness.

The tensile specimens had a 4mm diameter and a gauge length equal to 22mm. Four of them are machined to position the joint at the middle of the gauge length. Four other specimens are machined in the bulk 4330V. The tensile tests were done on a MTS hydraulic testing machined equipped with a 100kN force cell at a strain rate equal to $7 \cdot 10^{-4} \text{s}^{-1}$. All these tests are performed under air and the strain of the specimens is measured with an MTS extensometer having a 12mm gauge length. At 250°C, the maximal temperature difference between the middle of the tensile specimen and its upper or its lower part is about 5°C.

Five KV impact toughness specimens are also machined at the middle of the mock-up inside the bulk 4330V steel. According to the orientation of the notch, the impact toughness tests performed hereby allow the quantification of the transverse impact toughness of the forged 4330V steel bar, which give generally the lower impact toughness value of forged materials. The specimens are tested on a 300J pendulum (two were tested at 20°C and three at 250°C). At 250°C, the time to brake the sample is about five seconds as it is required in the NF EN ISO 148-1 standard.



Figure 17: 4330V/4330V mock-up to evaluate the mechanical properties of the 4330V and 4330/4330V joint after a HIP done at 1160°C/102MPa/3h and post heat treatments to harden the 4330V steel to the required hardness.

Figure 18 shows the tensile stress-strain curves of the bulk 4330V and the 4330V/4330V joint recorded at 20°C and 250°C. The stress is the recorded force (F) divided by the initial cross section of the tensile specimen (S_0). These curves enable to obtain the yield strength (YS) for a strain equal to 0,2%, the tensile strength (TS) and the total elongation of the specimen (A). These values are tabulated in the Table 5. The tempering heat treatment performed twice at a moderate temperature for two hours after the oil quench allows to obtain a very strong material with a yield strength of about 1400MPa at 20°C and about 1200MPa at 250°C. The elongation reaches only about 10% at 20°C that is less than the elongation of the 4330V material in the as received state (14%). At 250°C, the total elongation of the steel reaches 14%.

The 4330V/4330V joint presents similar value to the bulk 4330V when the tensile specimens were machined near the centre of the mock-up (about 15mm away the stainless steel canister used to perform the HIP diffusion bonding between the two-4330V pieces). In this region, the joint is sound and has very few residual porosities that could come from the Nital etching (Figure 19). For those located more closely to the stainless steel canister, the rupture occurs at the joint without any necking of the gauge length (Figure 20). It indicates a weak bonding between the two-4330V pieces in this region of the assembly. Unfortunately, no detailed analyses and no new experiments were done to understand this lack of bonding in our work. These results show that the second design imagined initially to manufacture the drill bit is not fully reliable at this stage of the study. Its use will need to erase a large part of the joint by machining which can be a problem during the manufacturing operations. For this reason we have focused our attention on the first design.

D2.9 Report on the development of materials and coatingsVersion:

Date: 25 January 2023

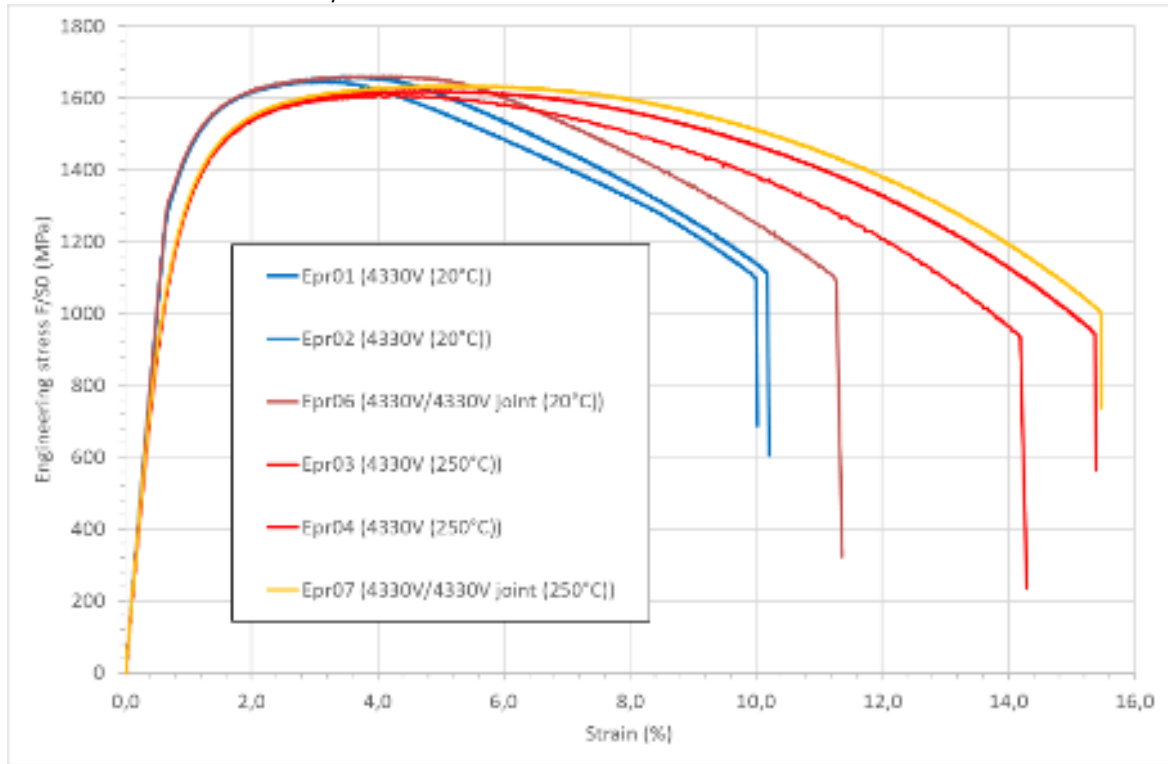


Figure 18: tensile stress-strain curves of bulk 4330V and 4330V/4330V joint at 20°C and 250°C.

Table 5: tensile properties of the bulk 4330V and 4330V/4330V joint at 20°C and 250°C after post HIP heat treatments

T	Specimen	State	Strain rate	TS	YS	A%	A % metrology	Z
(°C)			(s-1)	(MPa)	(MPa)	(%)	(%)	(%)
20	Forged bar	As received	unknown	1579	1137	14	14	56
	Epr01	Bulk	7,00E-04	1648	1410	9,7	9,4	53,2
	Epr02	Bulk	7,00E-04	1662	1412	9,9	9,7	50,2
	Epr05	Joint	7,00E-04	Rupture at the joint				
	Epr06	Joint	7,00E-04	1662	1417	11,2	11,0	52,3
250	Epr03	Bulk	7,00E-04	1609	1222	14,2	14,0	62,1
	Epr04	Bulk	7,00E-04	1623	1229	15,1	15,0	60,4
	Epr07	Joint	7,00E-04	1636	1219	15,1	15,1	57,0
	Epr08	Joint	7,00E-04	Rupture at the joint				

To complete the tensile results obtained above, impact toughness tests have been done. Table 6 gives the mean impact toughness of the 4330V steel at 20°C and 250°C and the Figure 21 shows the broken specimens after the tests. The values obtained at 20°C and 250°C are low but we do not have experimental feedbacks nor standard requirements associated to our application to judge these values.

D2.9 Report on the development of materials and coatingsVersion:

Date: 25 January 2023

Table 6: KV impact toughness of 4330V steel after post HIP heat treatments (oil quench after 1h at 870°C and tempering done twice at 330°C for 2h).

Bulk 4330V	20°C	250°C
Mean impact toughness (J)	27	42



After etching with 2% Nital. The arrows indicate the localization of the joints

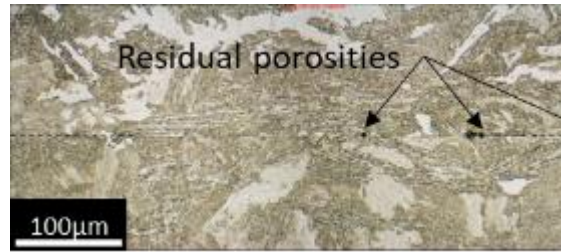


Figure 19: 4330V/4330V interface close to the centre of the mock-up.

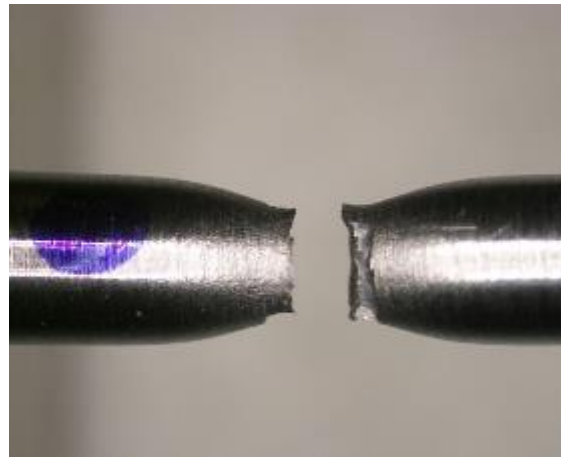
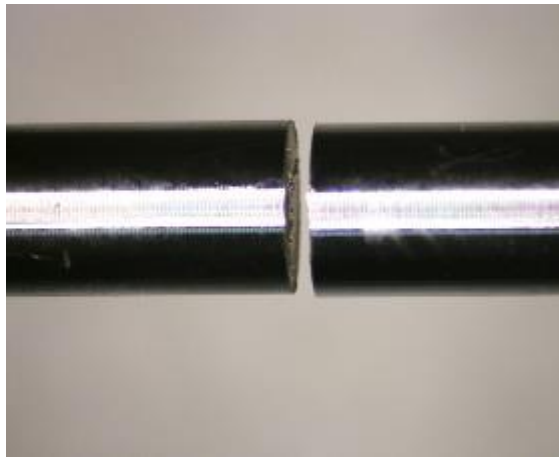


Figure 20: photographs of the broken tensile specimens to test the mechanical behaviour of the 4330V/4330V joint at 20°C. The left photograph shows the specimen located close to the canister whereas the right photograph shows the specimen located close to the centre of the mock-up. Similar observations at 250°C.

Date: 25 January 2023

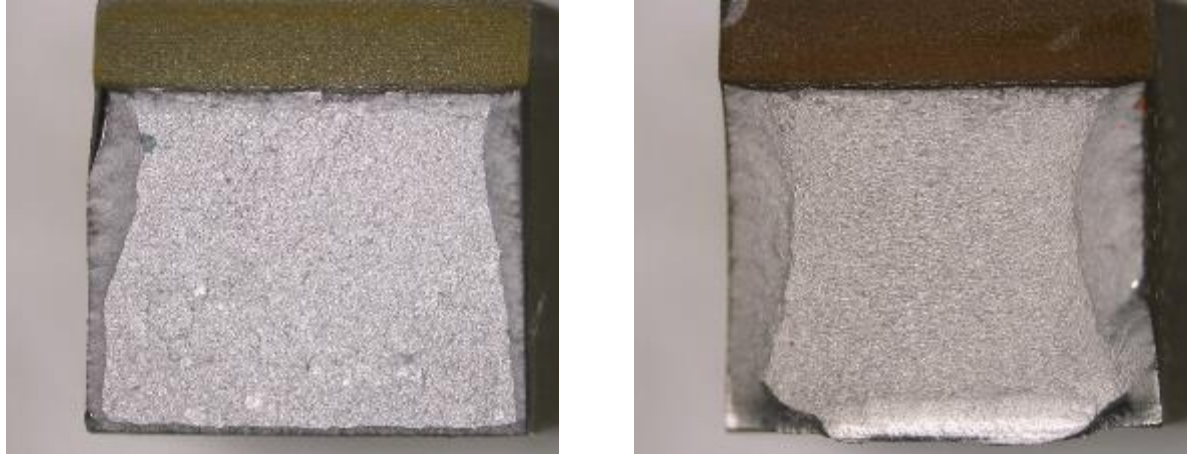


Figure 21: photographs of impact toughness specimens broke at 20°C (left) and 250°C (right).

Fabrication of mock-ups to study the HIP bonding of WC-Co to 4330V steel

HIP joining of WC-Co/4330V without metallic interlayer (reference mock-ups)

In order to study direct HIP bonding of cemented tungsten carbide to the 4330V low-alloyed carbon steel, both designs described in Figure 16 are manufactured without metallic interlayer. The assembly sequence of each design is presented in Figure 22. Following the assembly of all the pieces inside the stainless steel canister and its evacuation, both mock-up are HIPed. Figure 23 gives the temperature and the pressure recorded during the HIP cycle.



Figure 22: fabrication of the two investigated designs without metallic interlayer (reference mock-ups)

D2.9 Report on the development of materials and coatingsVersion:

Date: 25 January 2023

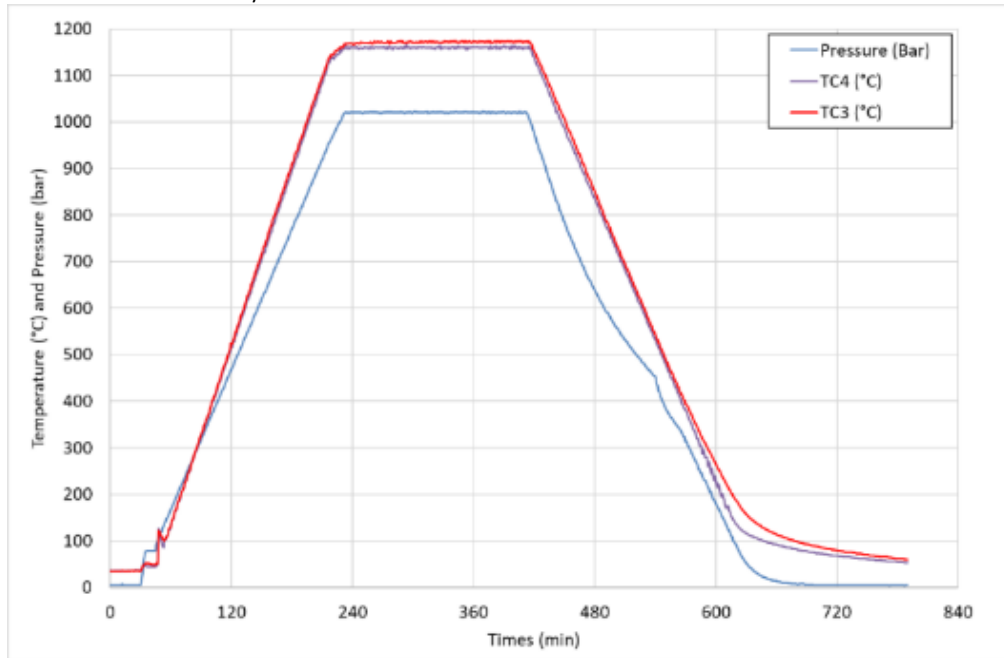
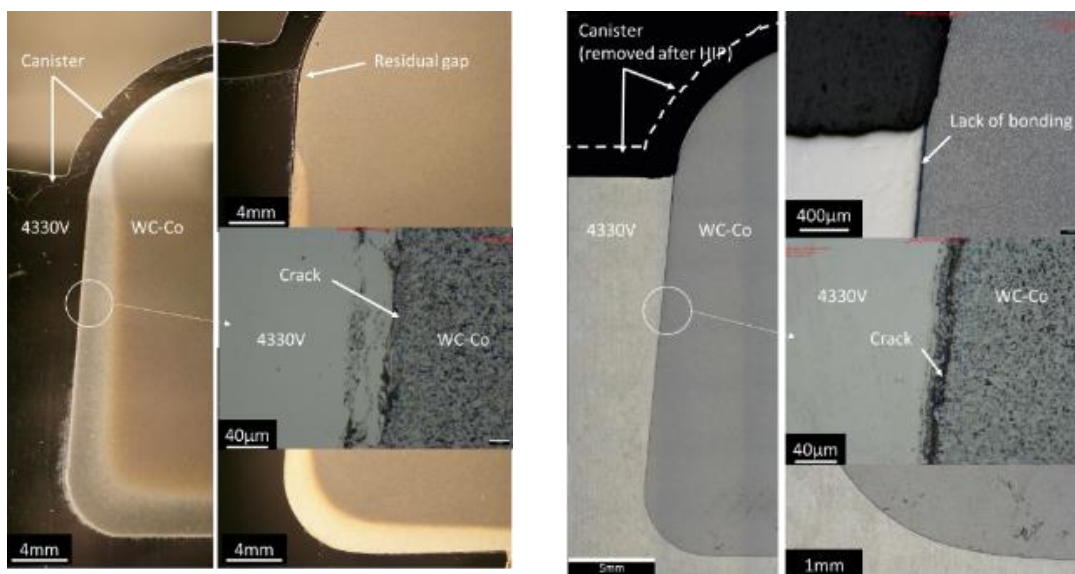


Figure 23: temperature and pressure recordings during the 1160°C/102MPa/3h HIP cycle of the reference mock-up.

Figure 24 shows the polished cross section of both designs after the HIP. For the first design, the simultaneous application of a high pressure and a high temperature plateau for several hours allows to close the majority of the initial gap that existed between the tooth and the steel. However, despite a good mechanical anchoring of the WC-Co tooth inside the steel due to its conical shape, cracks are visible at the WC-Co/4330V interface. Similar observations are made on the second design. The cracks propagate inside the WC-Co tooth very close to the WC-Co/4330V interface as is seen in Figure 25. SEM analyses reveal that the cracks propagate inside a cobalt-depleted region due to its diffusion inside the 4330V steel leaving behind a brittle WC band.



First design after HIP

Second design after HIP

Figure 24: polished cross sections of both designs after HIP.

Date: 25 January 2023

HIP joining of WC-Co/4330V with metallic interlayer

Following the fabrication of the reference mock-ups, new ones are manufactured by putting a metallic interlayer between the WC-Co tooth and the 4330V steel. This interlayer is metallurgically compatible with the WC-Co cermet and the steel. Its low yield strength brings flexibility to the assembly. Its thickness is different for the two investigated designs: for the first design, its thickness is 0.5mm (laminated foil) while it is 0.1mm for the second design (electrodeposition coating). With these interlayers, the assembly sequence is similar to that described in Figure 22 and the HIP cycle is 1160°C/102MPa/3h.

After HIP, the polished cross sections of the WC-Co/4330V joints made with the 0.1mm and the 0.5mm thick interlayers are presented in Figure 27. With both of them, the WC-Co/Interlayer/4330V joint is good and free from cracks, which is a good point. SEM analyses show a simultaneous diffusion of Co inside the interlayer and the interlayer inside the Co cement of the tooth. They show also that 0.1mm is sufficiently thick to avoid the diffusion of iron from the steel to the WC-Co (see Figure 28 and Figure 29).

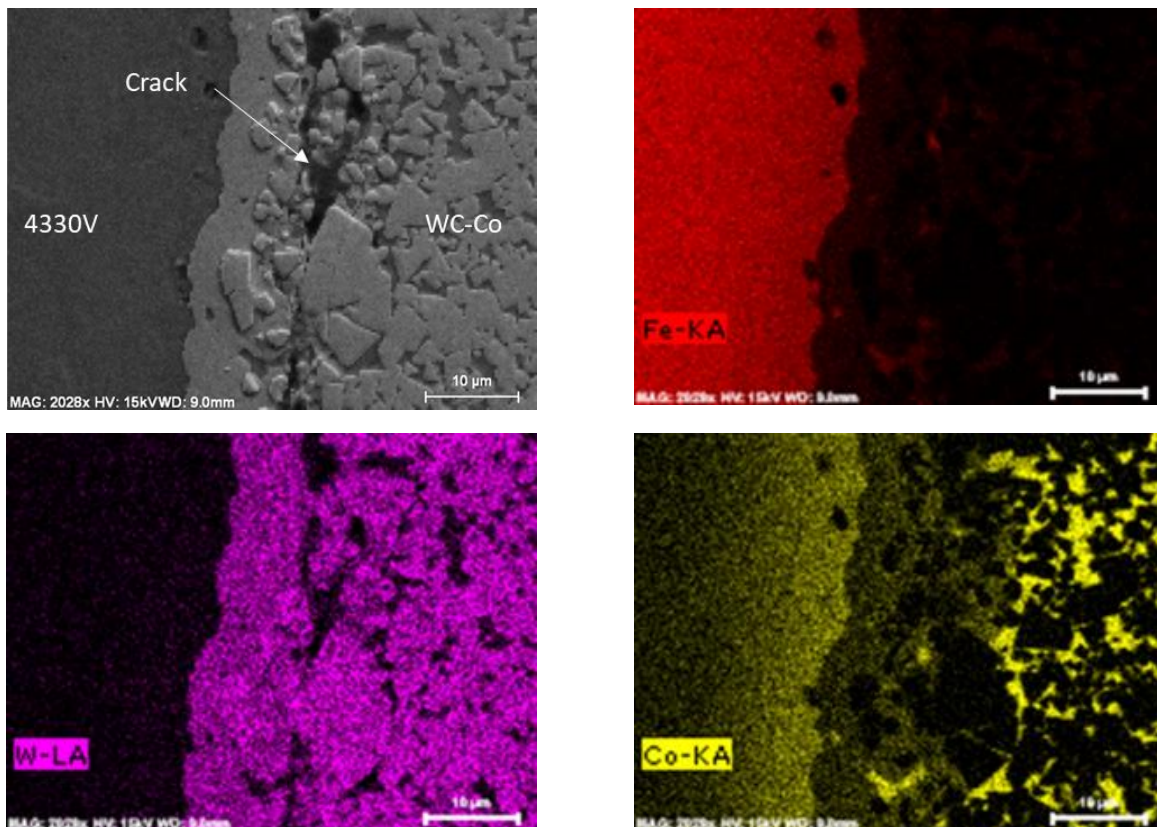
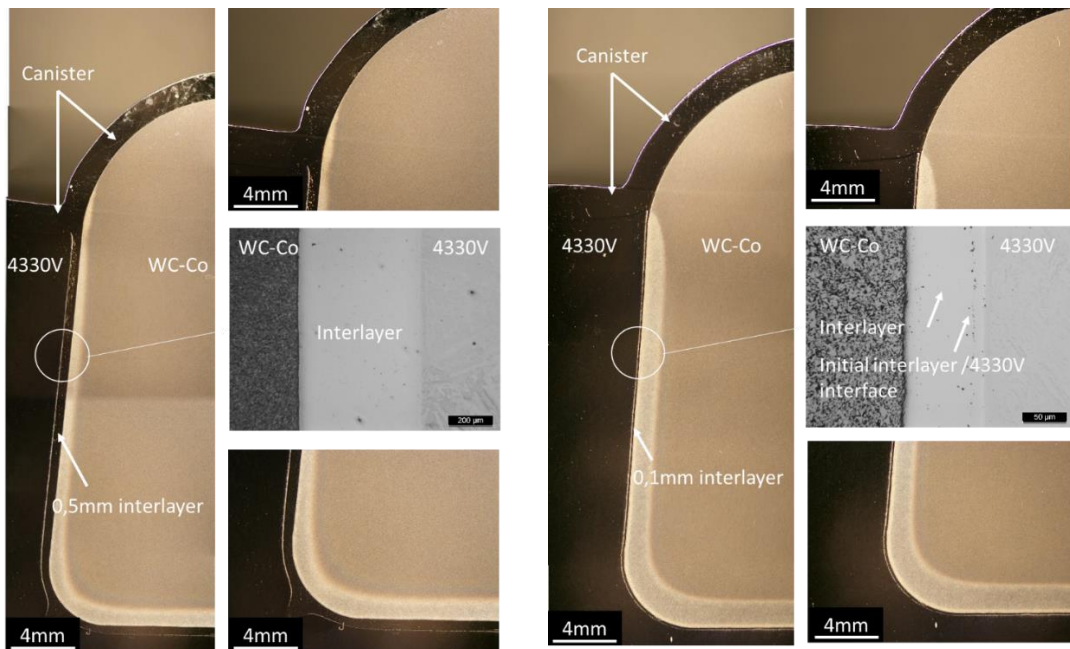


Figure 25: WC-Co/4330V interface in the second design after HIP and SEM FEG analyses

Date: 25 January 2023



Figure 26: fabrication of the two investigated designs with the 0.1mm and the 0.5mm thick interlayers



First design after HIP with 0.5mm thick interlayer

Second design after HIP with 0.1mm thick interlayer

Figure 27: polished cross sections of both designs made with 0.1mm and 0.5mm thick interlayers after HIP.

Date: 25 January 2023

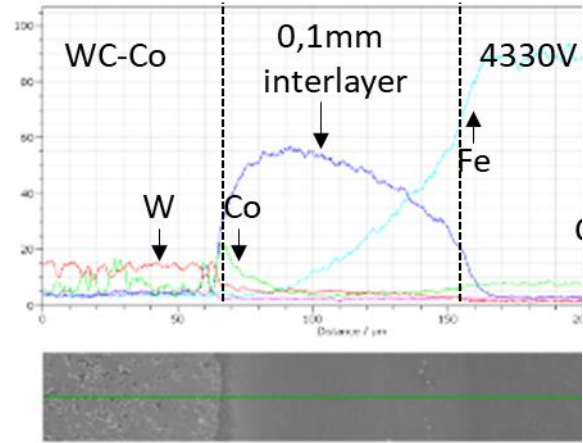
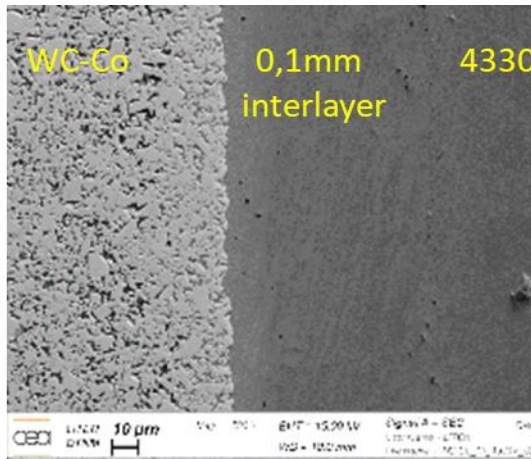


Figure 28: SEM EDX analysis performed on the WC-Co/0.1mm interlayer/4330V joint after HIP.

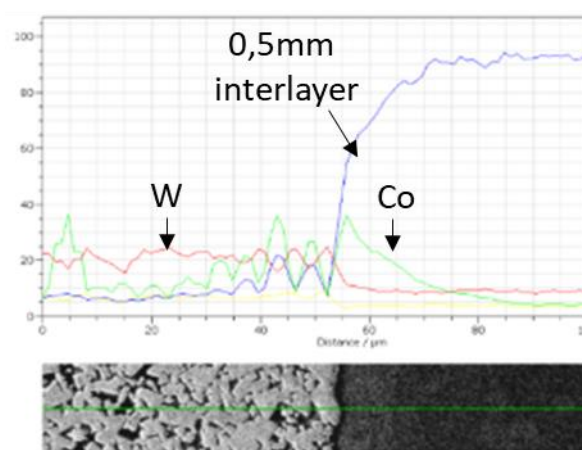
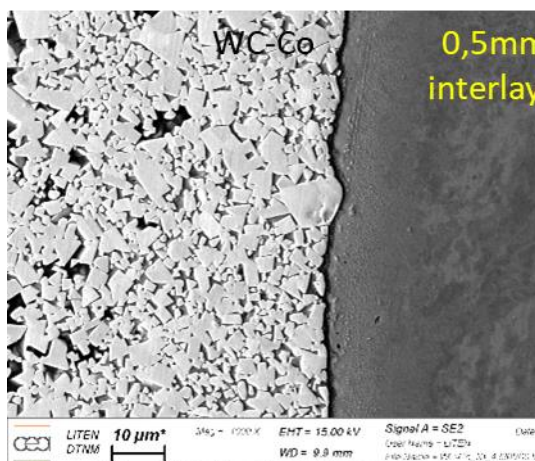
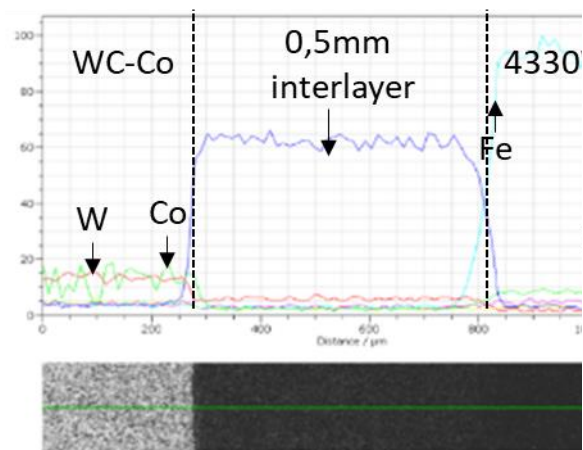
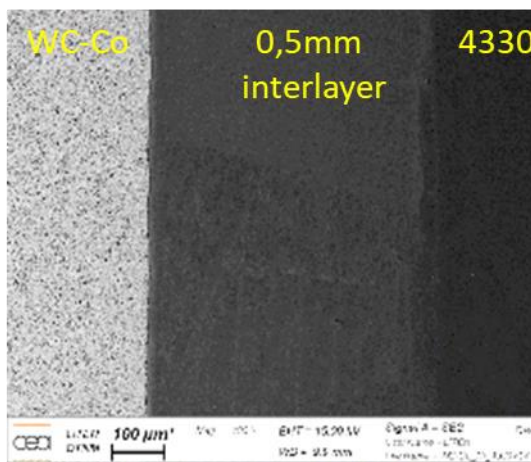


Figure 29: SEM EDX analyses performed on the WC-Co/0.5mm interlayer/4330V joint after HIP

WC-Co/interlayers/4330V joints after post HIP heat treatments

To verify the integrity of the WC-Co/interlayers/4330V joints after the post-HIP heat treatments, new mock-ups similar to those manufactured previously are made. One is made with a 0.1mm thick

D2.9 Report on the development of materials and coatingsVersion:

Date: 25 January 2023

interlayer and two others with a 0.5mm thick interlayer. These two last mock-ups are made with an as received tooth and a polished tooth to see if the mean surface roughness of the tooth is important or not. Their fabrication is similar to those described previously and after a HIP done at 1160°C/102MPa/3h, the mock-ups are heat treated at 870°C for 1h, oil quenched and tempered twice at a moderate temperature to reach the required hardness. Following the tempering heat treatments, the metallographic samples are extracted by spark discharge machining as it was done previously.

Figure 30 shows a polished cross section of the WC-Co/4330V joints made with the 0.1mm thick interlayer. On this photograph, cracks are visible on the two conical vertical regions of the WC-Co tooth. Enlargement of these regions shows that the cracks are located inside the WC-Co tooth very close to the WC-Co/interlayer interface (Figure 31).

Figure 32 shows the polished cross sections of two WC-Co tooth/4330V joint made with the same 0.5mm thick interlayer. The left photograph is a joint made with an as received WC-Co tooth (high surface roughness) while the right photograph is a joint made with a polished tooth (very low surface roughness). In both cases, the WC-Co/4330V joints are good and free of cracks (see Figure 33) indicating that both types of surface give a similar result from a HIP bonding point of view. However, cracks appear inside the teeth indicating that the weak point of this assembly is the cermet itself. However, these cracks seem to be smaller in the polished tooth than in the as received tooth but no numerical study was made to verify this point.

These results show that the soft interlayers allow fabrication of strong WC-Co/4330V joints, which resist to the post HIP heat treatments especially the oil quenching operation. However, due to the high strength of these joints, high stress is transferred to the WC-Co which then fails. We assume that the oil quench is the operation that leads to the highest stress in the assembly and we decide to replace it by a gas quench to see if a lower cooling rate can avoid the failure of the WC-Co tooth.

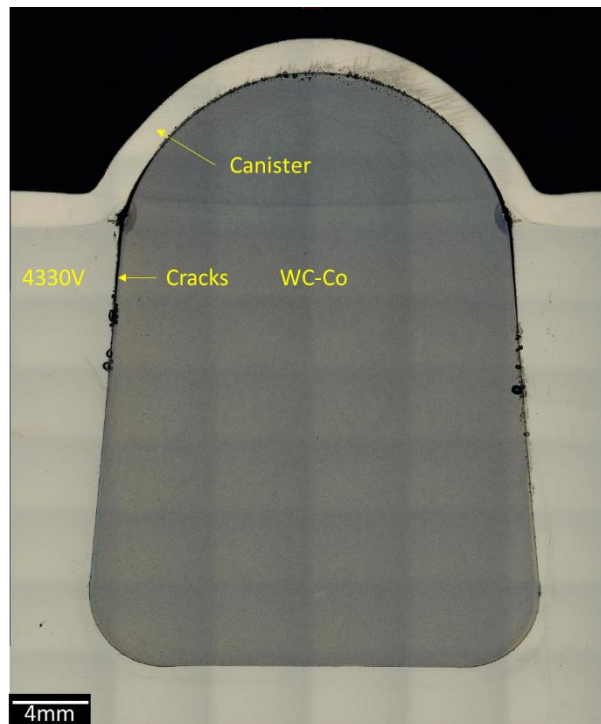


Figure 30: polished WC-Co tooth/4330V joint made with the 0.1mm thick interlayer.

Date: 25 January 2023

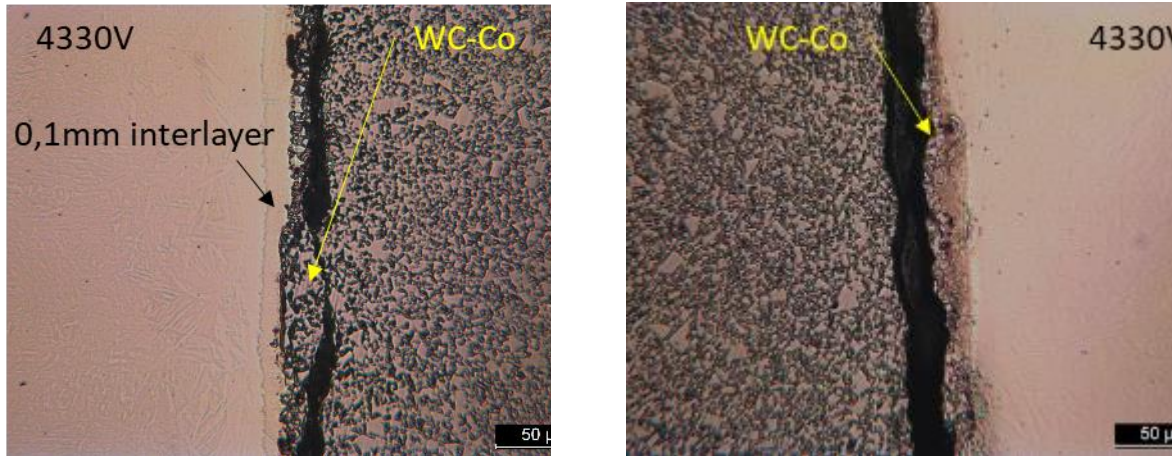


Figure 31: optical observations of the WC-Co/0.1mm interlayer/4330V joint after post-HIP heat treatments showing that the crack is located inside the WC-Co tooth very close to the WC-Co/interlayer interface.

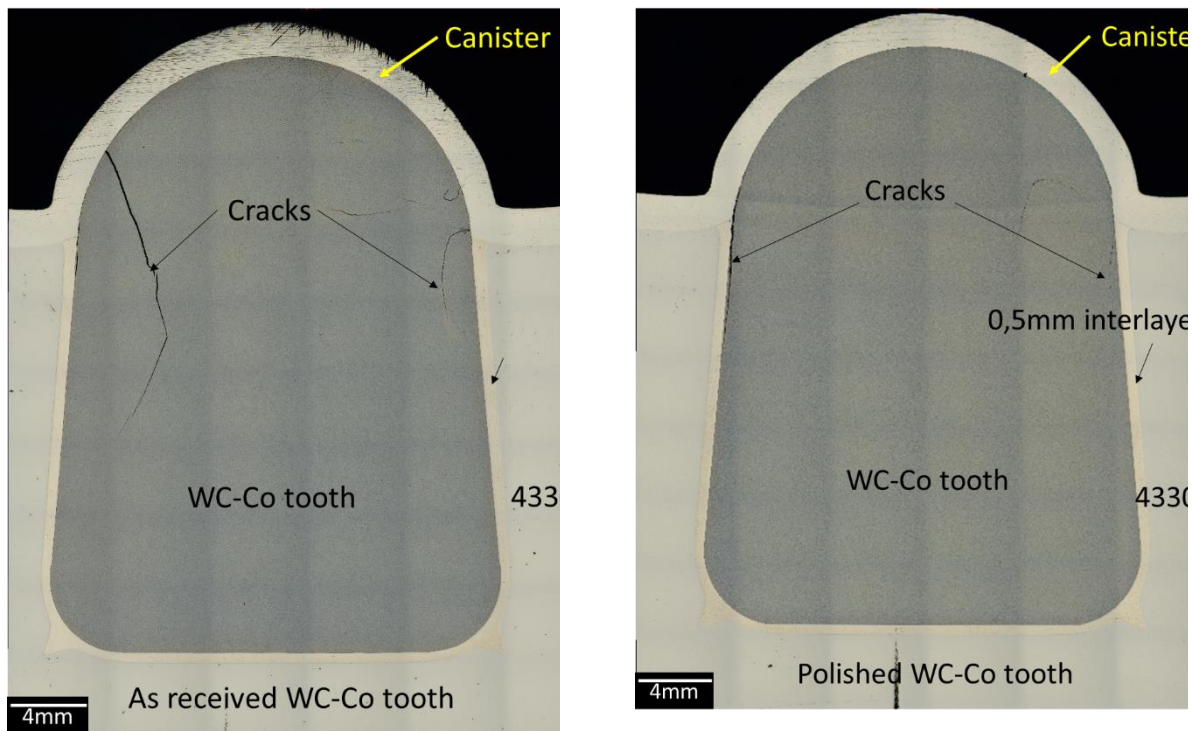


Figure 32: polished WC-Co tooth/4330V joint made with a 0.5mm thick interlayer. The left photograph is a joint made with an as received WC-Co tooth (surface with a high roughness). The right photograph is a joint made with a polished WC-Co tooth.

Date: 25 January 2023

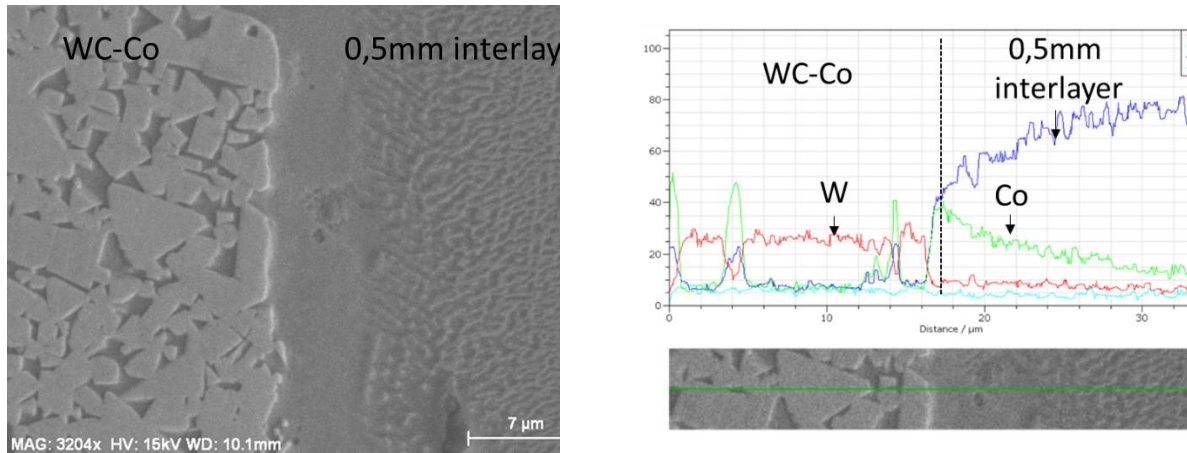


Figure 33: SEM photograph and EDX analysis of the WC-Co/0.5mm interlayer/4330V joint after post HIP heat treatments

Influence of quenching cooling rate on crack resistance of WC-Co tooth.

According to the previous results, we modified the post HIP heat treatments by replacing the oil quench by a gas quench in order to cool slowly the WC-Co/4330V joint. A new WC-Co/4330V mock-up is fabricated with a 0.5mm thick interlayer. HIP joining is performed classically at 1160°C/102MPa/3h then, the mock-up is austenitized at 870°C for one hour and gas quench instead of oil quench. This modification significantly reduces the cooling rate of the joint without changing the final hardness of the steel that fulfils the final hardness requirement.

Then, the mock-up is cut in two and one cross section is polished to observe the tooth and the joint (see Figure 34). The photographs show that the joint is good and free of defects but unfortunately, two large cracks are visible inside the WC-Co tooth. As the cooling rate of the mock-up measured during the gas quench is much slower than during the oil quench, we assume that the quenching rate is not the only parameter to take into account to avoid the failure of the WC-Co tooth. At the measured cooling rate, the WC-Co tooth does not fail. Therefore, the cracks could be due to the martensitic transition in the the 4330V steel.

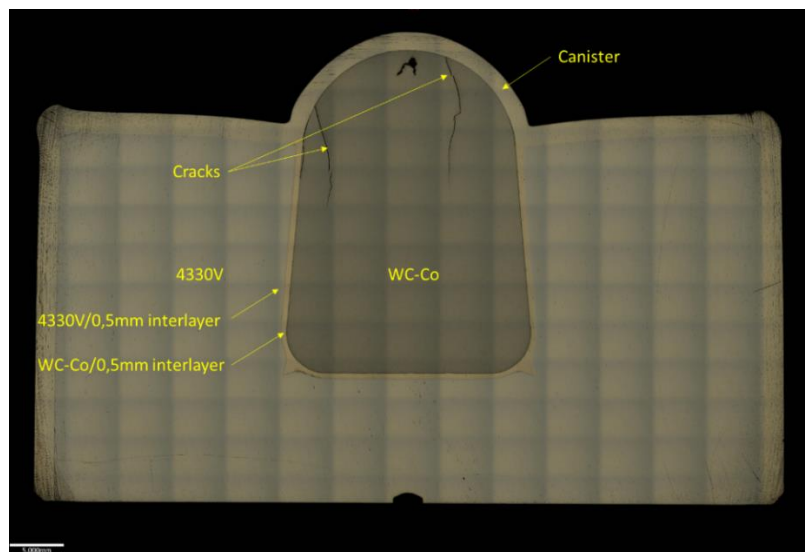


Figure 34: polished cross section of the mock-up made with HIP at 1160°C/102MPa/3h and then gas quench and temper twice at 330°C during 2h.

D2.9 Report on the development of materials and coatingsVersion:

Date: 25 January 2023

To limit the stress due to this transition, it could be interesting to slowly cool the WC-Co/4330V joint between Ms and Mf. This is done classically in industry by quenching the steel inside a salt bath set just above the martensitic start temperature. Then the steel is cooled under calm air. This experimental verification has not been done in WP2.4 but it will be done in WP5. Nevertheless, we can propose a HIP manufacturing route according to this hypothesis. This route will include the following points:

- A HIP at 1160°C/104MPa/3h to bond the WC-Co tooth to the 4330V steel with a 0.5mm Ni interlayer.
- An austenitization heat treatment of the WC-Co/4330V joint at 870°C for 1h
- A gas quench from the austenitization temperature down to a temperature above Ms to cool the WC-Co/4330V joint at a slower rate than the oil quench operation.
- A thermalization of the joint above Ms during several minutes and then a cooling of the WC-Co/4330V joint under calm air to pass slowly the martensitic transition between Ms and Mf.
- Finally, a tempering heat treatment to reach the 4330V steel required hardness

Conclusion

Experimental investigations to propose a manufacturing route of a drill bit using HIP as a technical solution to bond the hard WC-Co inserts onto the bit head was carried out in this task. To perform this work, the CEA has selected two materials. The cemented tungsten carbide for the hard inserts and the low alloy steel for the head and the shank of the drill bit.

The hard WC-Co inserts were manufactured by Element Six with coarse WC grains and a cobalt content equal to 15Wt. % to have a good compromise between the wear resistance and the impact toughness. HIP was used after sintering to densify totally the cemented tungsten carbides. Their conical shape was designed to improve their anchoring inside the steel.

The steel is a vacuum arc remelted low alloyed 4330V steel manufactured by Carpenter. In the as received state, its mean hardness is 251HV30. After HIP, the hardness rises to 358HV30 but it is still lower than the required hardness for our application. To reach this value, HIPed 4330V shall be heat-treated by performing an austenitization heat treatment at 870°C for one hour that ends by a quench in a hot oil bath. At this stage, the steel is fully martensitic and its hardness is 588HV30. To reduce its hardness to the required level, several tempering heat treatments were performed at different temperatures for a fixed duration equal to 2 hours. The hardness requirement is obtained by tempering twice the steel at a moderate temperature for two hours. A reduction of the steel cooling rate by making a gas quench instead of an oil quench does not change drastically the hardness of the 4330V steel at every stage of the post HIP heat treatments but it has a strong influence on the mechanical integrity of the WC-Co tooth.

The diffusion bonding of the WC-Co tooth to the 4330V steel was studied by considering two designs to manufacture the drill bit. In the first design, the tooth is placed inside a borehole machined inside the steel. The borehole diameter is slightly larger than the diameter of the tooth and HIP is used to close the residual gap between the tooth and the steel. In the second design, the tooth is sandwiched between two 4330V steel pieces and its anchoring inside the steel is obtained by joining the two 4330V pieces by HIP. In the first design, HIP parameters shall be defined to insure a full filling of the residual gap by the steel. In the second design, HIP parameters shall be defined to insure a good diffusion bonding between the two 4330V pieces. Adaptive DOE and adaptive metamodeling were not used in this study to define the manufacturing design of the drill bit because very few information regarding the mechanical behaviour (tensile, creep, rupture criteria...) of the selected steel and WC-Co cermet were available in the literature to conduct efficiently this study in the allowed time.

Concerning the HIP parameters, our study evaluated only one set of parameters, which are commonly used in industry to HIP low alloy steel alloys. These parameters are a temperature equal to 1160°C and a pressure equal to 102MPa for three hours. According to our experimental results, these

D2.9 Report on the development of materials and coatingsVersion:

Date: 25 January 2023

parameters enables to close the residual gap between the tooth and the steel in the first investigated design. In the second design, they enables to bond correctly the two 4330V steel pieces together but the metallographic examinations of the joints show residual porosities and a lack of bonding close to the stainless steel canister. Tensile tests performed on the joint in this region lead to a quick break of the specimens without necking of the gauge length. Far way the stainless steel canister, the joint is sufficiently good and the tensile behaviour of the joint is as good as the bulk material at both investigated temperatures (20°C and 250°C). The use of the second design to fabricate the drill bit appears thus to be less reliable than the first design.

Direct bonding of the WC-Co tooth to the 4330V steel at 1160°C/102MPa/3h, leads to a weak interface whatever the investigated design. Metallographic examinations show that the tooth are well anchored inside the steel after HIP but cracks are visible inside the WC-Co very close to the WC-Co/4330V interface. Metallographic examinations show that cracks propagate in a WC-Co region impoverished by cobalt (and thus enriched by brittle WC) due to its diffusion inside the iron matrix during the HIP cycle. The use of a selected interlayer made directly on the surface of the tooth by electrodeposition (thickness of about 0.1mm) or by bending a foil (thickness equal to 0.5mm) enables to fabricate a WC-Co/4330V joint free of crack after the HIP. However, the application of the post heat treatments described above leads to the rupture of the WC-Co tooth. This result means that the WC-Co/interlayer/4330V joint is stronger than the cermet itself. To reduce the thermal stress of the WC-Co that could lead to its failure, a new mock-up was manufactured by replacing the oil quenching by a gas quenching. Unfortunately, metallographic examinations performed after the tempering heat treatments showed several cracks inside the WC-Co tooth indicating that the reduction of the cooling rate at a much lower rate than that measured during the oil quench is not the only parameter to take into account to avoid the failure of the teeth. At this stage of the project we assume that the martensitic transition of the 4330V steel has a significant influence on the stress of the teeth and thus on their failure. To limit the stress to this transition we propose to stop the quenching at a temperature above Ms and then, to cool slowly the joint under calm air before doing the final tempering heat treatment. A HIP manufacturing route that follows this suggestion was proposed in this report. It will be tested in the WP5.

Task 2.5: Development of diffusion bonding process for tool joint and drill stabiliser

Introduction

Task 2.5 is dedicated to the fabrication of the tool joint and the drill stabilizer by HIP. The tool joint is the enlarged and threaded end of a drill pipe (Figure 35). This part of the drill string is fabricated separately from the pipe body and welded by rotary friction welding onto the pipe at a manufacturing facility. The tool joints provide high strength and high pressure threaded connections that have to be robust to survive the rigors of drilling and the numerous cycles of tightening and loosening at threads. For these reasons, tool joint is made with steel that has a higher strength than the steel used for the pipe body. However, despite the high hardness of steel, tool joints suffer from galled thread, thread damage and metallic shoulder damage that can have an effect on the tightness of the metal/metal connection. To avoid these problems and improve the tool joint lifetime, we have proposed to reinforce the tool joint shoulder with a higher strength alloy that could has a higher hardness than the 4140 steel after tempering.

D2.9 Report on the development of materials and coatingsVersion:

Date: 25 January 2023

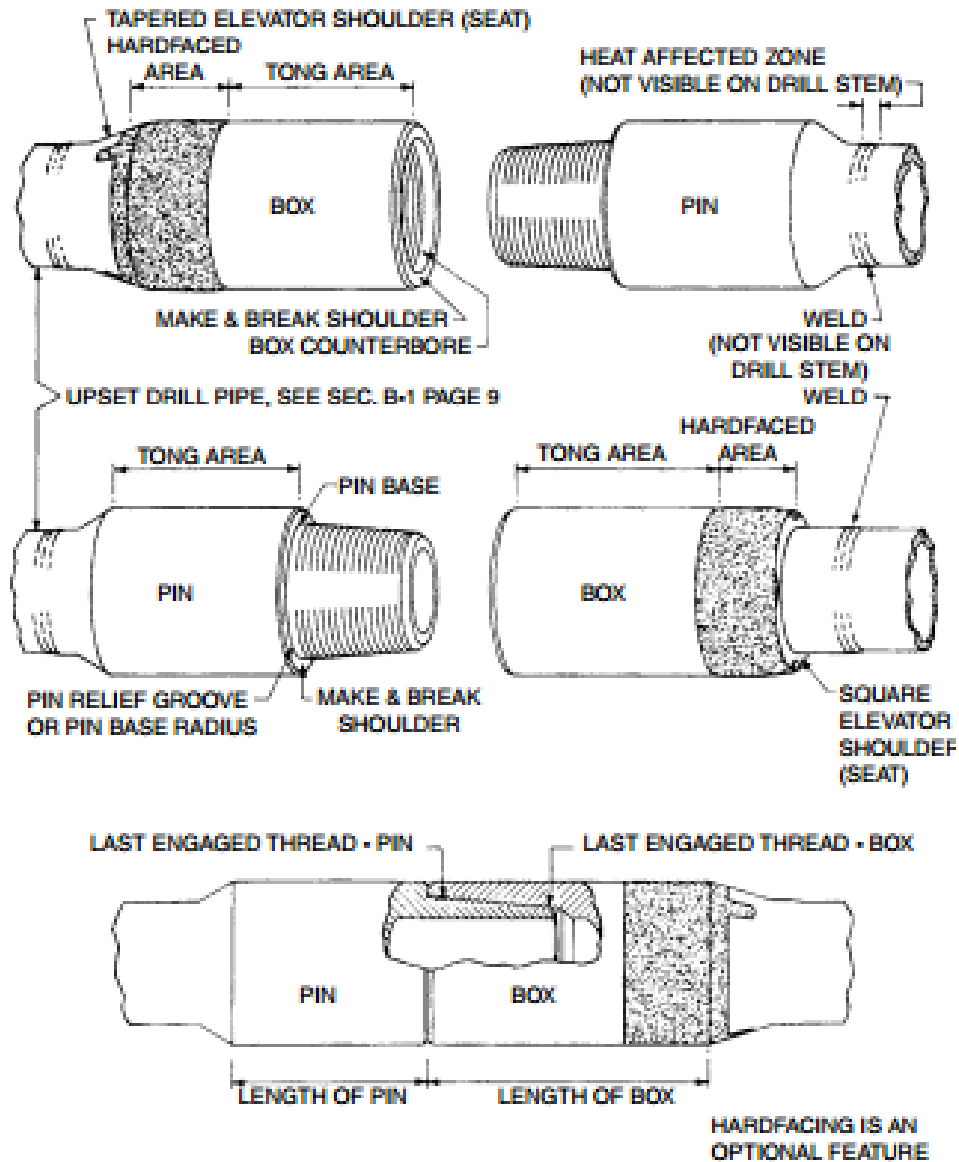
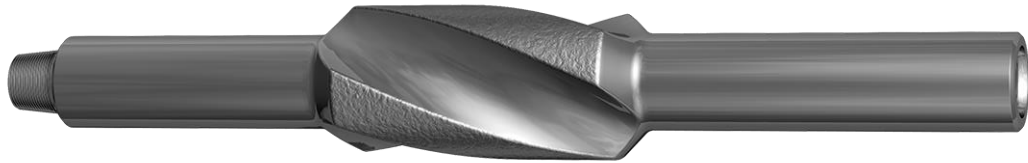


Figure 35: drawing of classical API tool joint used in oil and gas industry.

The drill stabilizer is a part of the down the hole equipment. It stabilizes the bottom hole assembly in the well to avoid side tracking or vibrations, and ensure the quality of the hole being drilled. It is composed of a hollow cylindrical body and stabilizing blades, both made of high-strength steel. The blades can be either straight or spiralled, and are typically hard-faced with cemented tungsten carbide inserts to improve their wear resistance. The hard facing operation is generally performed by hand torch brazing or by LASER cladding but both techniques heat the steel and affect its final strength.

Several types of drilling stabilizers are used. While integral stabilizers (fully machined out of a single piece of steel) tend to be the norm, other types can be used such as replaceable sleeve stabilizers or welded blades stabilizers (Figure 36).

Date: 25 January 2023



Integral stabilizer



Stabilizer with replaceable sleeve



Stabilizer with welded blades

Figure 36: examples of several types of stabilizer manufactured by JA oilfield [6]

As for the tool joint, we propose to improve the lifetime of the stabilizer by bonding, onto the external diameter of the drill pipe, blades made with high strength alloys. We will also explore the anchoring of very high strength WC-Co inserts onto one of the best high strength alloy by hot isostatic press (HIP) as it is developed in Task 2.4 to manufacture the drill bit.

Steel and high strength alloys grades

Following our bibliographic research, we propose to use an AISI 4140 steel grade to manufacture the tool joint and the stabilizer. To perform the development work program, a $\Phi 79\text{mm}$ 4140 round bar was purchased in normalized condition and the Table 7 gives its chemical composition. Vickers hardness measurements indicate that the mean hardness of the bar in the as received state is 230HV30.

For the high strength alloys, we focus our attention on a Fe-Ni-Co alloy and a Ni-Cr-Mo alloy. The Fe-Ni-Co alloy has a hardening heat treatment compatible with the hardening heat treatment of the 4140 steel and we purchased a $\Phi 76\text{mm}$ bar of this grade to perform the development work programme. The Ni-Cr-Mo alloy has a strength that depends only on its chemical composition and we purchased a 5mm thick plate to perform the experiments.

D2.9 Report on the development of materials and coatingsVersion:

Date: 25 January 2023

Table 7: chemical composition of the 4140 bar purchased to perform the work development programme.

4140 Grade	Chemical composition (Wt. %)							
	C	Mn	Mo	Si	S	P	Cr	Ni
Chemical standard	0.37-0.44	0.65-1.10	0.15-0.25	0.15-0.35	0,04mx	0,03mx	0.75-1.20	0.25mx
As received	0.42	0.91	0.21	0.23	0.005	0.012	1.02	0.07

Development of HIP bonding process parameters to bond the high strength alloys to the 4140 steel grade

Fabrication of mock-ups

To develop the HIP bonding process between the 4140 steel and the selected high strength alloys, we manufactured several mock-ups. Two mock-ups were made without anti diffusion interlayer in order to observe and document the diffusion of carbon from AISI 4140 steel towards both high strength alloys during an 1160°C/102MPa/3h HIP cycle. They are the reference mock-ups. Three other mock-ups were made with the same HIP cycle by adding 0.25mm, 0.5mm and 1mm thick interlayers between the 4140 pieces and the high strength alloys pieces to limit their carburization. The selected interlayers are metallurgically compatible with the materials to bond. All the HIPed mock-ups are presented in Figure 37.

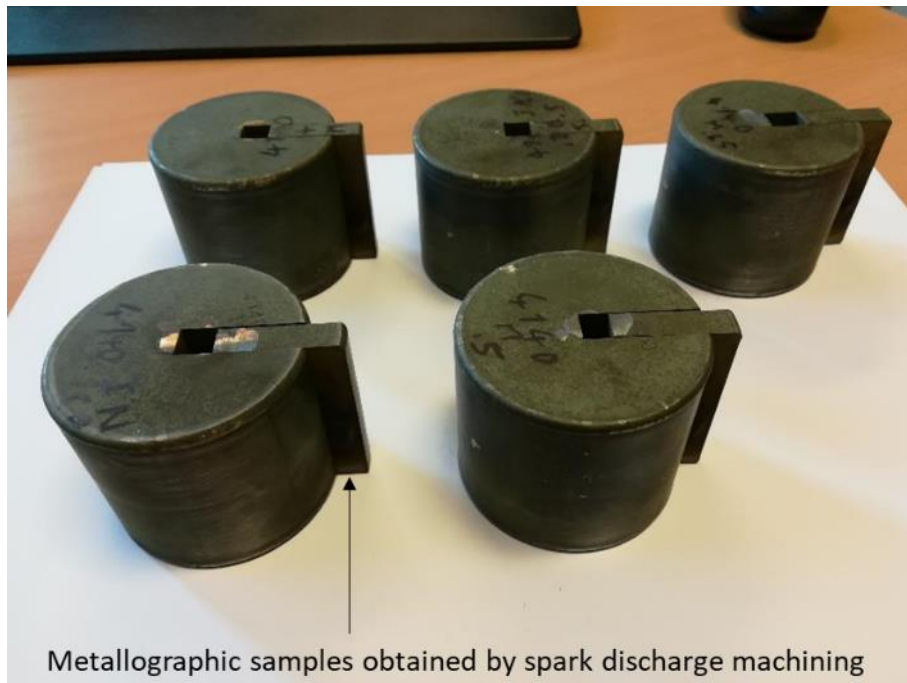


Figure 37: 4140/FeNiCo and 4140/NiCrMo/4140 joints after the HIP cycle done at 1160°C/102MPa/3h. Each mock-up was cut by spark discharge machining to extract a metallographic sample.

Date:

25 January 2023

Metallographic examination of HIP diffusion bonded joints

Samples extracted from each mock-up are polished and then observed by optical microscopy. Hardness measurements are also made on the polished samples to quantify the carburization of both high strength alloys. The images of the 4140/FeNiCo joints made with and without an interlayer are presented in Figure 38. Without an interlayer, we notice a strong carburization of the high strength alloy that expands to about 2mm through its grain boundaries. This carburization is correlated with a strong increase in Vickers hardness close to the 4140/FeNiCo interface (Figure 39). By assuming that carbon diffuses only during the high temperature plateau of the HIP cycle, it is possible to estimate the length of its diffusion in an austenitic Fe-C alloy (Equation 1). At 1160°C (1433K), the calculated diffusion length is about 1.6mm, which is fully in accordance with the value found experimentally.

$$\text{Equation 1 } L = \sqrt{Dt} \text{ with } D = D_0 e^{-\frac{Q}{RT}}, D_0 = 0.2 \text{ cm}^2/\text{s} \text{ and } Q = 135 \text{ kJ/mole}$$

The use of anti-diffusion metallic interlayers leads to a reduction in the carburization of the FeNiCo alloy without avoiding it totally. With a 1mm thick interlayer, optical and Vickers hardness measurements show that the carburization depth can be reduced down to 0.6mm. The use of a new 1mm thick interlayer having a higher nickel content than the previous one (interlayer N° 2) enables a further reduction in the carburization depth to 0.4mm (see Figure 40). In this last case, we note that, far away from the HIPed joint, the high strength steel has a higher hardness (346 HV30) than the 4140 steel (310 HV30).

The images of the 4140/NiCrMo alloy joints made with and without interlayer are presented in Figure 41. We observe immediately that the carburization of the NiCrMo alloy is much lower than the FeNiCo alloy because of its higher nickel content. As for the FeNiCo alloy, the addition of a metallic interlayer having a high nickel content (interlayer N°2) allows reduction of the carburization of the NiCrMo alloy (see Figure 42) but we do not notice a clear variation on the Vickers hardness measurements done across the interface (see Figure 43).

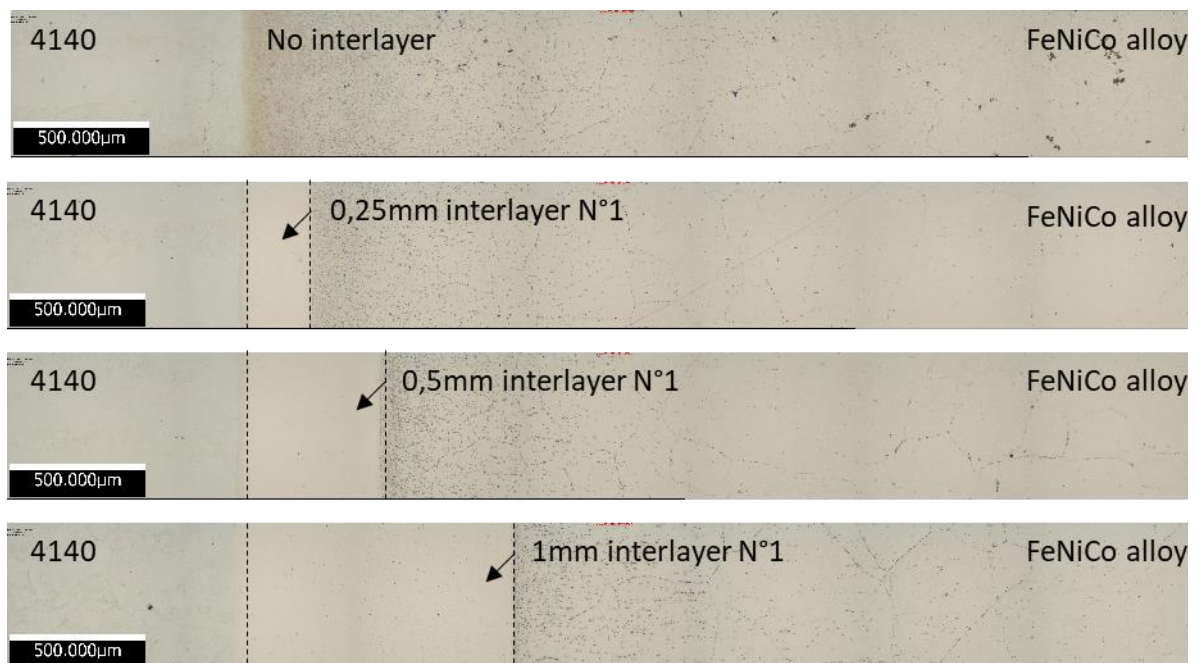


Figure 38: images of the 1160°C/102MPa/3h HIP diffusion bonded joints between 4140 steel and FeNiCo with and without interlayers

D2.9 Report on the development of materials and coatingsVersion:

Date: 25 January 2023

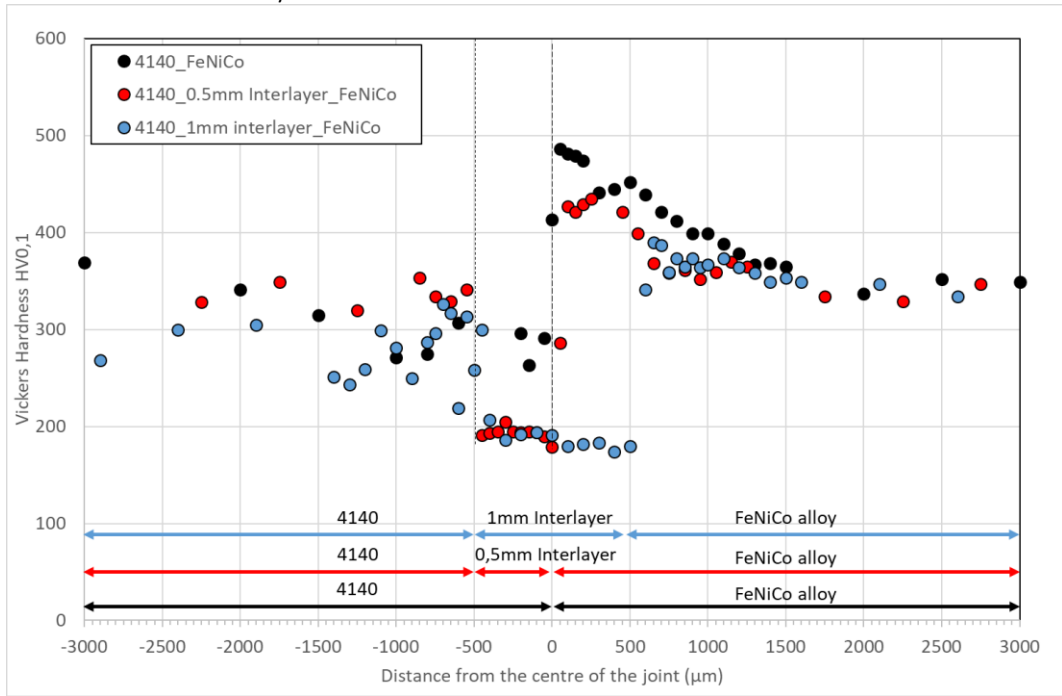


Figure 39: Vickers hardness measurements performed on 4140/FeNiCo alloy joints made with and without interlayer.

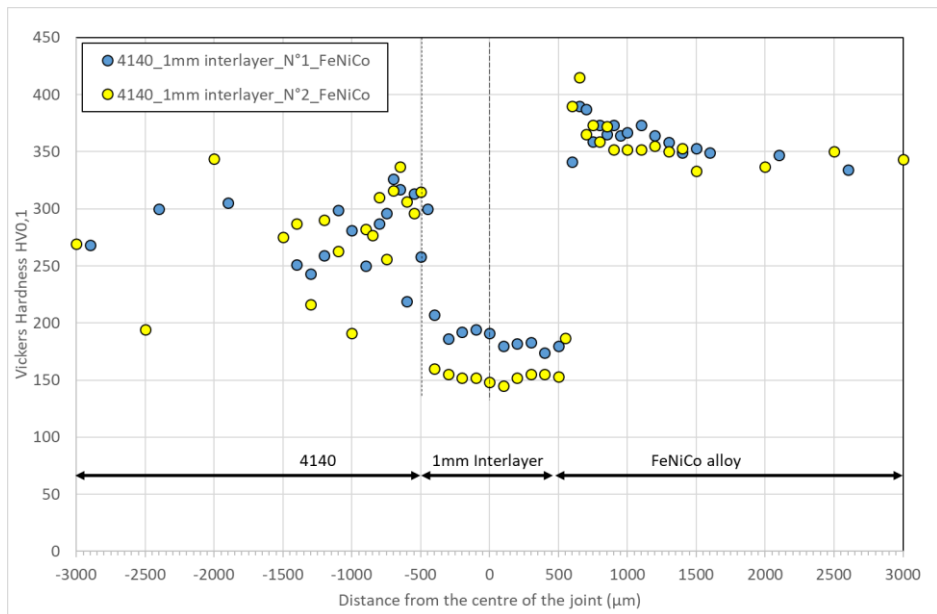


Figure 40: Vickers hardness measurements performed on 4140/FeNiCo alloy joints made with two different interlayers having the same thickness (1mm) but a different nickel content. The interlayer having the higher content nickel but the lower hardness is the most efficient to limit the diffusion of carbon inside the high strength alloy.

D2.9 Report on the development of materials and coatings Version:

Date: 25 January 2023

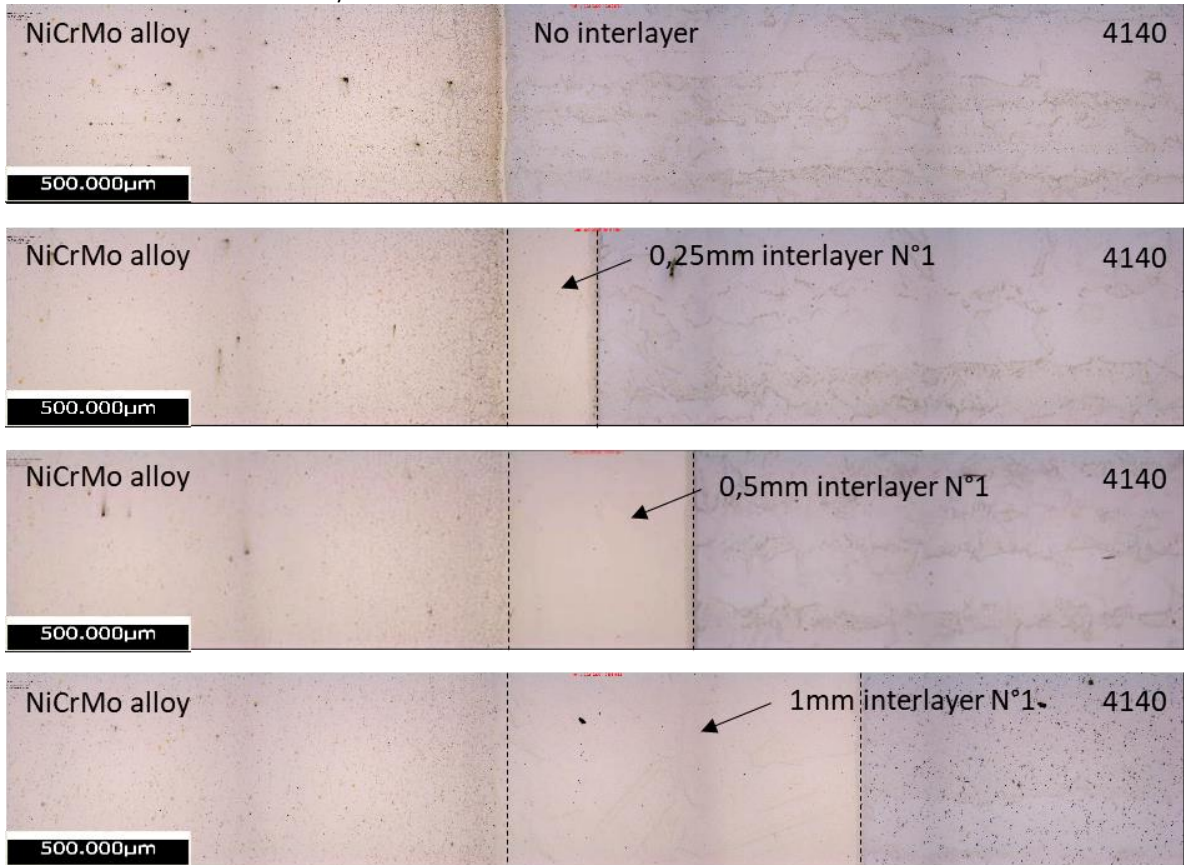


Figure 41: images of the 1160°C/102MPa/3h HIP diffusion bonded joints between 4140 steel and NiCrMo with and without interlayers

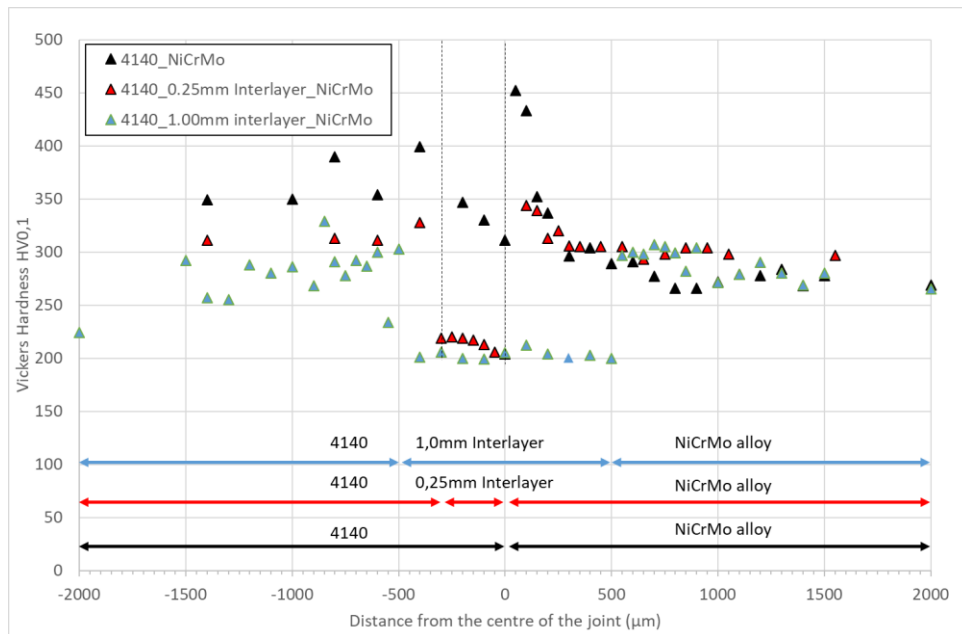


Figure 42: Vickers hardness measurements performed on 4140/NiCrMo alloy joints made with and without interlayer.

Date:

25 January 2023

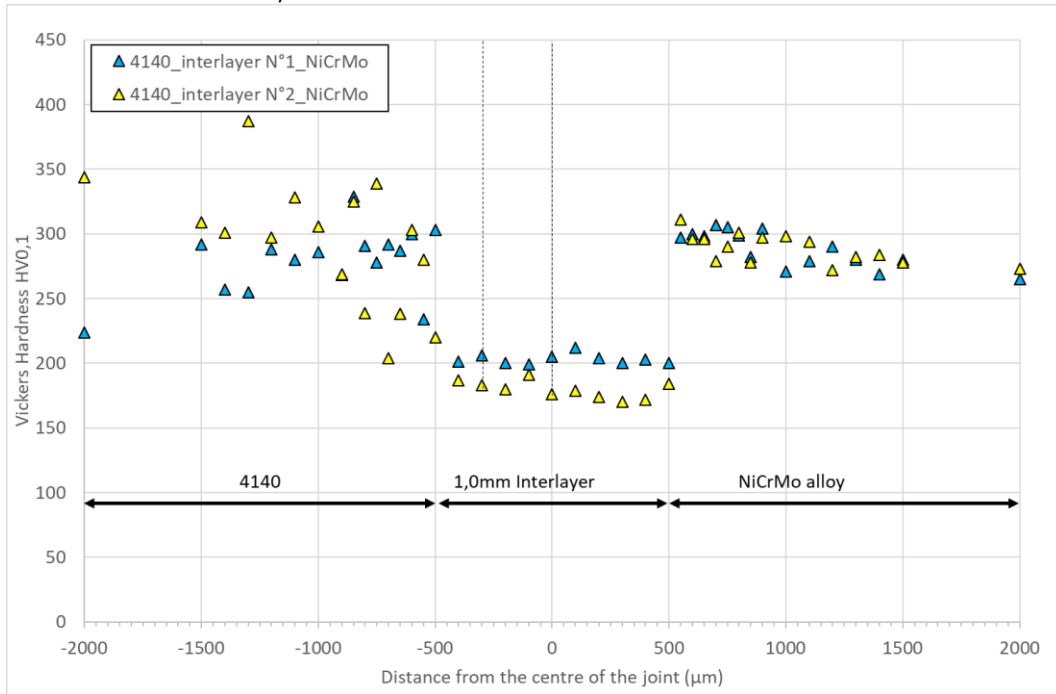


Figure 43: Vickers hardness measurements performed on 4140/NiCrMo alloy joints made with two different interlayers having the same thickness (1mm) but a different nickel content.

Influence of a reduced HIP temperature on the carburization of the FeNiCo alloy

To further reduce the carburization of the FeNiCo alloy during the HIP cycle, the temperature was decreased from 1160°C to 1100°C keeping the pressure and the duration of the plateau at respectively 102MPa and 3h. Figure 44 shows the polished cross section of the 4140/FeNiCo joints made at the two different HIP temperatures with the same interlayer (interlayer N°2 with a thickness equal to 1mm). According to these images, the carburization of the FeNiCo is still present at 1100°C but it seems lower than at 1160°C. Vickers hardness measurements performed with 0.1kg across the joints confirm this tendency with a slightly lower hardness of the FeNiCo alloy HIPed at 1100°C instead of 1160°C (see Figure 45). A further reduction of the HIP temperature would have been interesting to implement in this programme to know if the carburization of the FeNiCo alloy continues at lower temperatures. But, due to the time duration of the task, it was decided preferably to mechanically test the joint performed with a 1mm thick interlayer at the two investigated temperature to compare their mechanical strength.

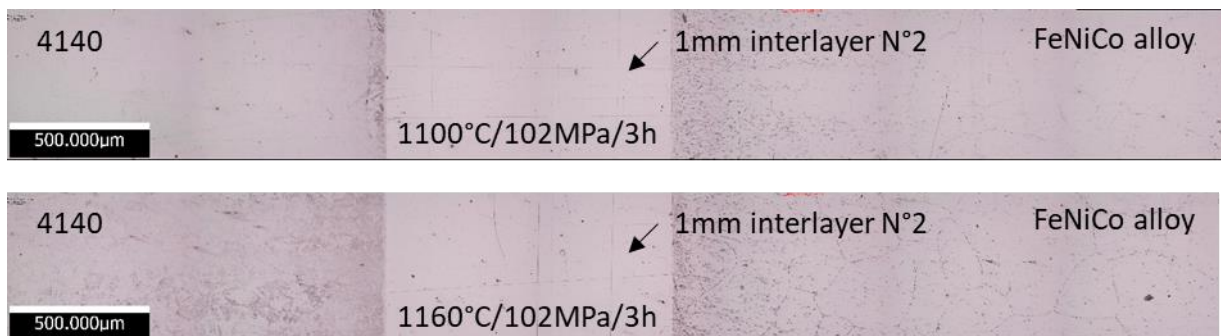


Figure 44: images of 4140/FeNiCo joints made at 1100°C/102MPa/3h and 1160°C/102MPa/2h with the interlayer N°2. The thickness of the interlayer is 1mm.

Date:

25 January 2023

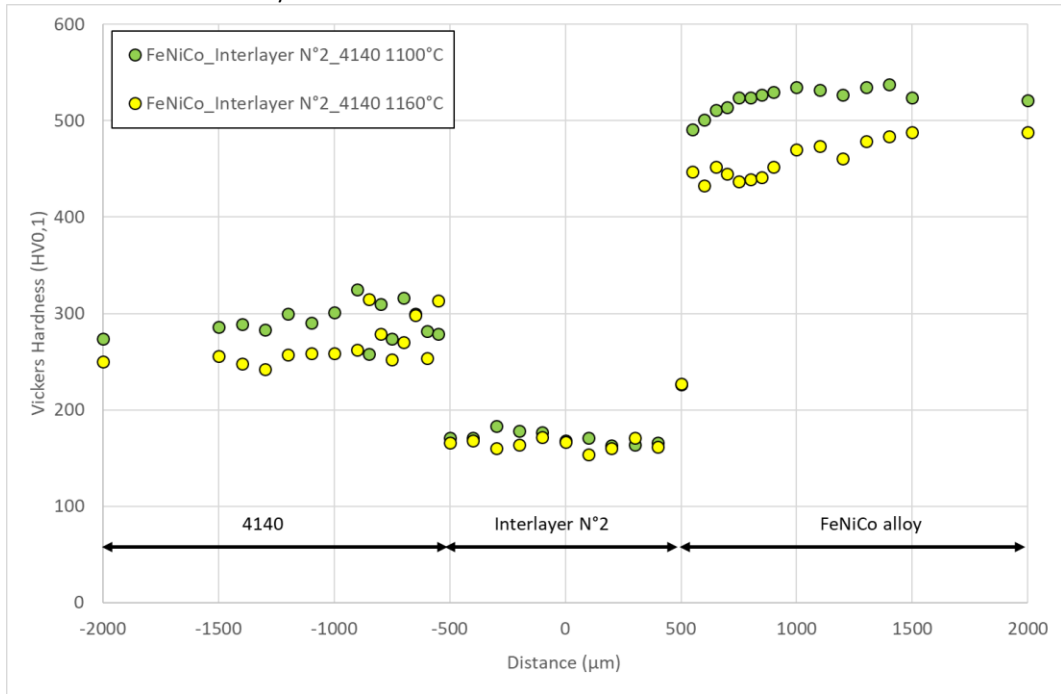


Figure 45: Vickers hardness measurements performed on the 4140/FeNiCo joints made with a 1mm thick interlayer (interlayer N°2) at 1100°C and 1160°C and post heat-treated to reach the 4140 required hardness.

Influence of post heat treatment on the hardness of the 4140 steel and the two high strength alloys

According to Chapter 8 of the API 5D standard, the hardness of the tool joint shall be in the range 300-350HV. The 4140 steel reaches this range of hardness after the HIP cycle (310HV30) but, as the cooling rate inside a HIP is low, it shall be subjected to an austenitization and a quench heat treatments to dissolve the brittle phases that appear during the slow cooling phase of the HIP cycle. Then, the steel is tempered at a fixed temperature to reach the required hardness.

To determine the best tempering temperature after the HIP, previously manufactured mock-ups are submitted to an austenitization heat treatment performed at 870°C for one hour and oil quenched in hot oil. Then, several tempering heat treatments are done at 540°C, 550°C and 625°C for 2 hours to harden preferentially the 4140 steel. At 540°C and 625°C, the Vickers hardness of the 4140 steel is outside the range of the API 5D standard but we obtain a Vickers hardness of about 340HV30 after a tempering treatment done at 550°C for 2h. With this tempering, the Vickers hardness of the FeNiCo alloy reaches 507HV30 while that of the NiCrMo alloy reaches only 181HV30. This value is much lower than the Vickers hardness of the 4140 steel so we do not select this material to reinforce the shoulder of the 4140 steel.

D2.9 Report on the development of materials and coatingsVersion:

Date: 25 January 2023

Table 8: Vickers hardness of the 4140, FeNiCo and NiCrMo alloys after the HIP and several post heat treatments including an austenitization heat treatment at 870°C for 1h, an oil quench and a final tempering heat treatment at different temperatures.

HV30 (HB)	After HIP at 1160°C/3h	870°C/1 + OQ + 540°C/2h	870°C/1 + OQ + 550°C/2h	870°C/1 + OQ + 625°C/2h
4140 steel	310 (294)	380 (360)	337 (319)	283 (269)
FeNiCo alloy	346 (328)	540 (508)	507 (49)	421 (398)
NiCrMo alloy			181 (181)	

Mechanical properties of 4140/4140, 4140/FENICO and 4140/NICRMO joints

Following the experiments to determine the best hardening heat treatment of the 4140 steel, several new mock-ups are manufactured to test the strength of the 4140/4140 and the 4140/FeNiCo joints. A 4140/NiCrMo joint is also manufactured at the same time for comparison. Table 9 gives the manufacturing conditions of each joint.

Following the fabrication of each joint, tensile specimens are machined inside each mock-up. The tensile specimens have a diameter equal to 4mm and a gauge length equal to 22mm. For the determination of the tensile strength of the joint at 20°C and 250°C (maximal operating temperature), the joint is located at the middle of the gauge length. All the tests are done on a hydraulic testing machine equipped with a 100kN cell force and an MTS extensometer having a gauge length equal to 12mm. All the tests are performed at $7 \cdot 10^{-4} s^{-1}$ and under air. KV impact toughness specimens are machined inside the 4140/FeNiCo mock-ups manufactured at 1100°C/102MPa/3h and 1160°C/102MPa/3h. The radius of the KV slit is located at the middle of the interlayer.

Table 9: manufacturing conditions of 4140/4140, 4140/FeNiCo and 4140/NiCrMo alloys

Type of joints	HIP conditions	Quenching conditions	Tempering conditions
4140/4140	1160°C/102MPa/2h	870°C/1h then oil quench	550°C/2h
4140/FeNiCo	1160°C/102MPa/2h With 1mm thick interlayer N°2	870°C/1h then oil quench	550°C/2h
4140/FeNiCo	1100°C/102MPa/2h With 1mm thick interlayer N°2	870°C/1h then oil quench	550°C/2h
4140/NiCrMo	1160°C/102MPa/2h With two 1mm thick interlayer N°1	870°C/1h then oil quench	550°C/2h

Date: 25 January 2023

Mechanical characterization of bulk 4140 and 4140/4140 joint

Figure 46 and Figure 47 give the tensile stress-strain curves of the bulk 4140 and the 4140/4140 joint at 20°C and 250°C. The stress is the ratio between the recorded force F and the initial cross section of the specimens S_0 . These curves enable to determine the yield strength, the tensile strength and the total elongation of the specimens at the investigated temperatures. These values are tabulated in the

Table 10.

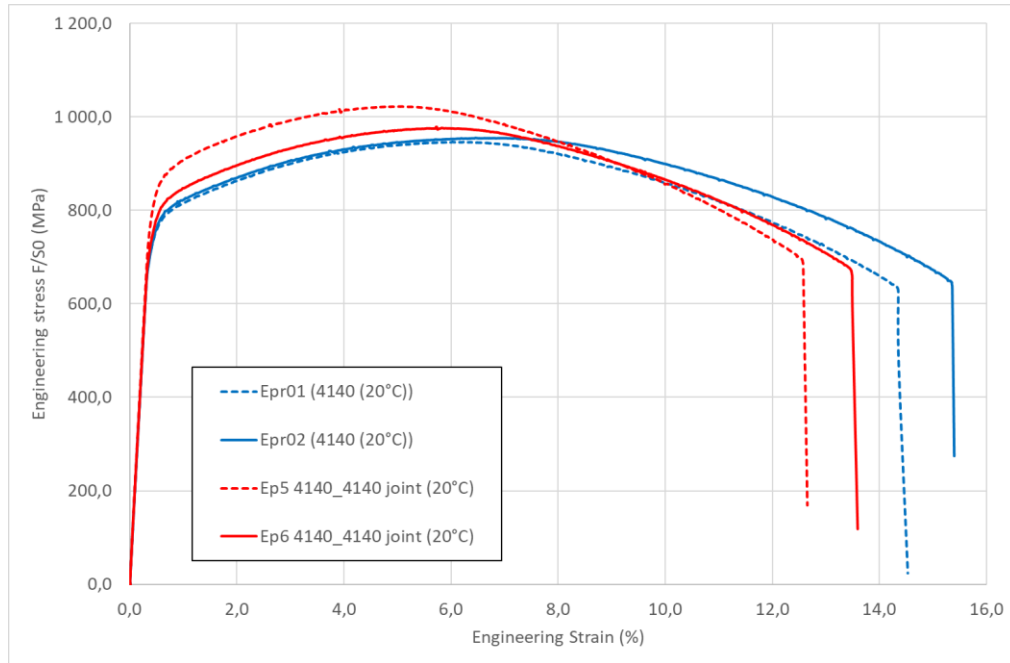
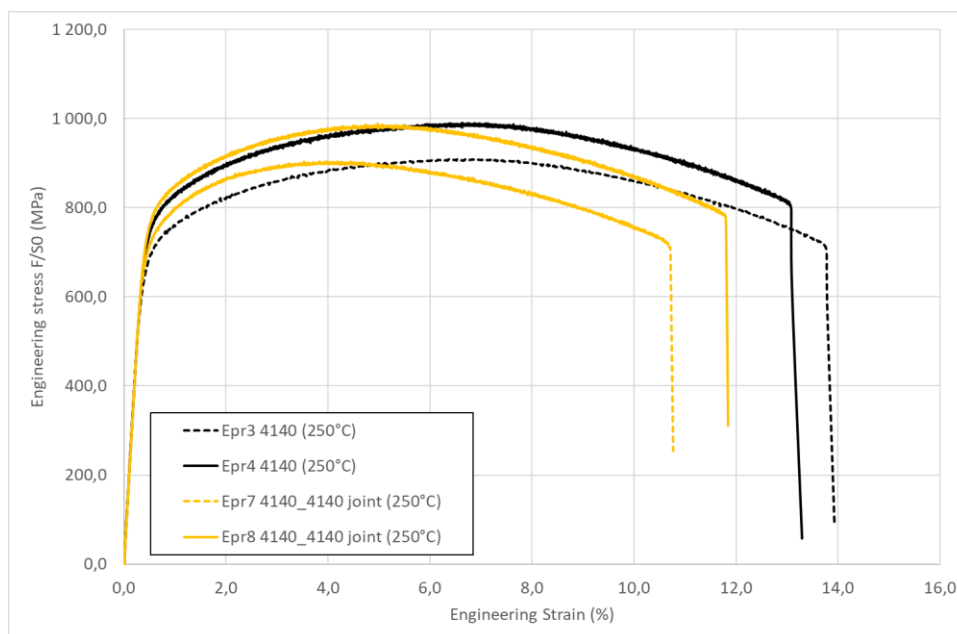


Figure 46: tensile stress-strain curves of 4140 steel and 4140/4140 joint at 20°C and $7 \cdot 10^{-4} s^{-1}$. The stress is the ratio between the recorded force F and the initial cross section of the tensile specimen S_0 .



D2.9 Report on the development of materials and coatingsVersion:

Date: 25 January 2023

Figure 47: tensile stress-strain curves of 4140 steel and 4140/4140 joint at 250°C and $7 \cdot 10^{-4} \text{s}^{-1}$. The stress is the ratio between the recorded force F and the initial cross section of the tensile specimen S_0 .

D2.9 Report on the development of materials and coatingsVersion:

Date: 25 January 2023

Table 10: tensile properties (tensile strength, yield strength at 0.2% elongation and total elongation A) of bulk 4140 and 4140/4140 joint at 20°C and 250°C at $7 \cdot 10^{-4}s^{-1}$.

T	Sample	State	E	Tensile Strength	Yield Strength	A%	A% metrology	Necking
(°C)			(MPa)	(MPa)	(MPa)	(%)	(%)	(%)
20	Epr01	Bulk	209774	947	776	14,5	14,6	57,8
	Epr02	Bulk	209981	955	782	15,3	15,5	57,9
	Epr05	Joint	217782	1022	864	12,6	12,6	56,6
	Epr06	Joint	211186	979	806	13,5	13,4	56,3
250	Epr03	Bulk	201568	910	701	13,9	14,2	45,3
	Epr04	Bulk	196704	992	770	13,3	12,7	41,9
	Epr07	Joint	199737	906	734	10,6	11,0	47,4
	Epr08	Joint	196015	988	793	11,7	11,4	43,2

According to these data, bulk 4140 steel HIPed at 1160°C/102MPa/3h and post heat treated to have a mean Vickers hardness of about 340HV30 has a yield strength close to 770MPa, a tensile strength close to 950MPa and a total elongation higher than 14%. These values decrease slowly at 250°C but they remain high. The 4140/4140 joint tested at 20°C and 250°C has a slightly higher yield strength and tensile strength than bulk 4140 but the elongation of the specimens is lower (down to 11%). Nevertheless, all the 4140/4140 specimens break outside the joint (see Figure 48) which means that the joint has similar mechanical properties to the bulk material.

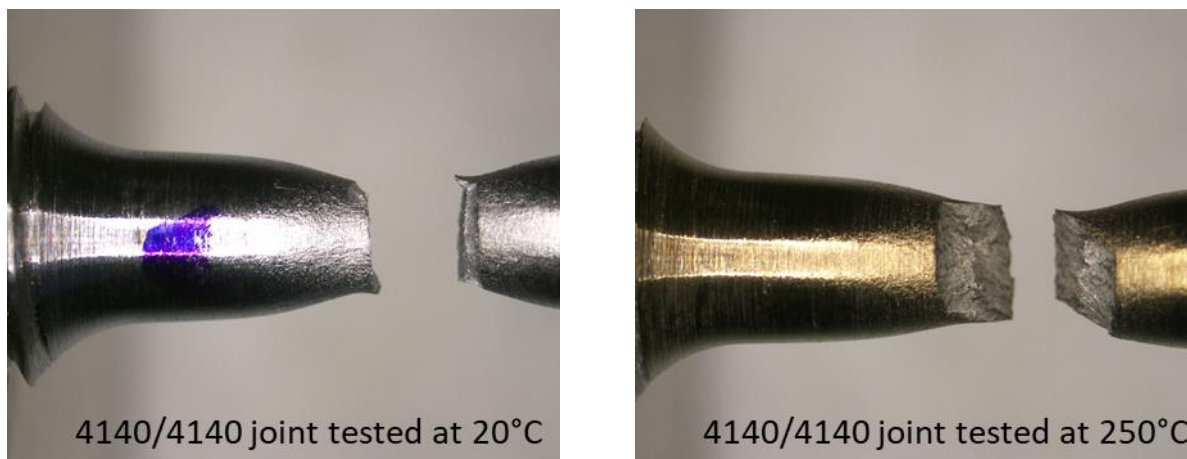


Figure 48: photographs of broken 4140/4140 joint tested at 20°C and 250°C at $7 \cdot 10^{-4}s^{-1}$. The rupture of the specimens occurs close to the connecting radius between the gauge length and the thread so, far away the joint.

D2.9 Report on the development of materials and coatingsVersion:

Date: 25 January 2023

KV Impact toughness tests are performed on the 4140 steel at 20°C and 250°C. The results are presented in the Table 11. At 20°C, the mean impact toughness is about 39J whereas it reaches 124J at 250°C. As no impact toughness requirements exist, it is difficult to say if these values are satisfactory or not.

Table 11: KV impact toughness of 4140 steel HIPed at 1160°C/102MPa/3h then oil quench and temper at 550°C for 2h

KV impact toughness (J)	20°C	250°C
4140 steel	39	124

Mechanical characterization of 4140/NiCrMo/4140 joint

Figure 49 shows the tensile stress strain curves of the 4140/NiCrMo/4140 joint recorded at 20°C and 250°C. Figure 50 shows the broken specimens. In every case, the rupture of the specimens occurs inside one of the two interlayers used to manufacture the mock-up and never at the joints. It indicates that the joints are stronger than the interlayers, which is a good point from a mechanical point of view. As the elongation of the specimens is mainly due to the strain of the NiCrMo alloy and the two interlayers, the true elongation associated to these three materials is about 30% (see Table 12). This value is much higher than the total elongation of the gauge length recorded first by the MTS extensometer and then the crosshead displacement of the hydraulic machine (about 13%). The comparison with the tensile stress-strain curves of the 4140 steel in Figure 49 shows that the mechanical properties of the 4140/NiCrMo/4140 joint is much lower at both investigated temperatures which is not a surprise because of the hardness of the NiCrMo alloy and the interlayer.

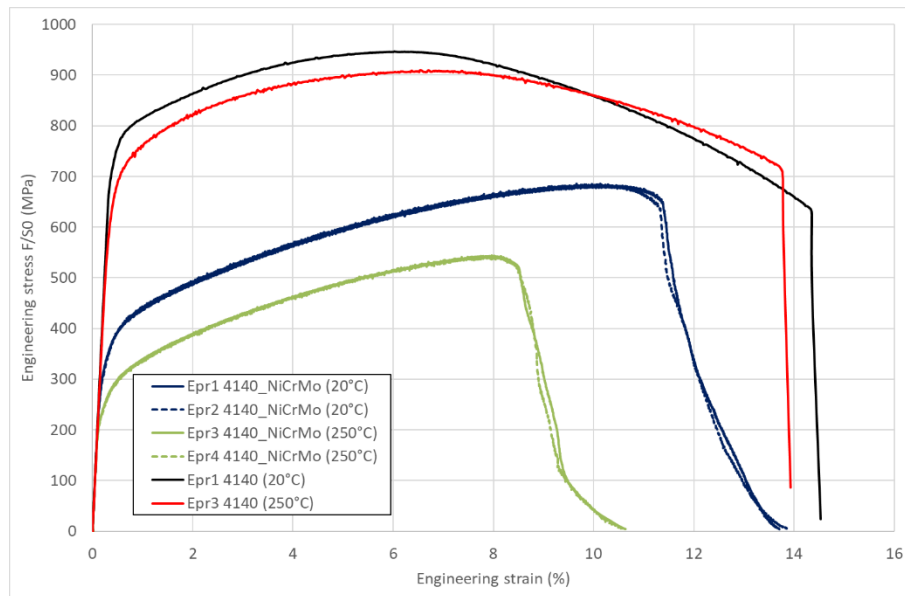


Figure 49: tensile stress-strain curves associated to the 4140/NiCrMo joints manufactured with 1mm thick interlayer N°1. Stress-strain curves recorded at 20°C and 250°C at $7 \cdot 10^{-4} s^{-1}$.

Date: 25 January 2023

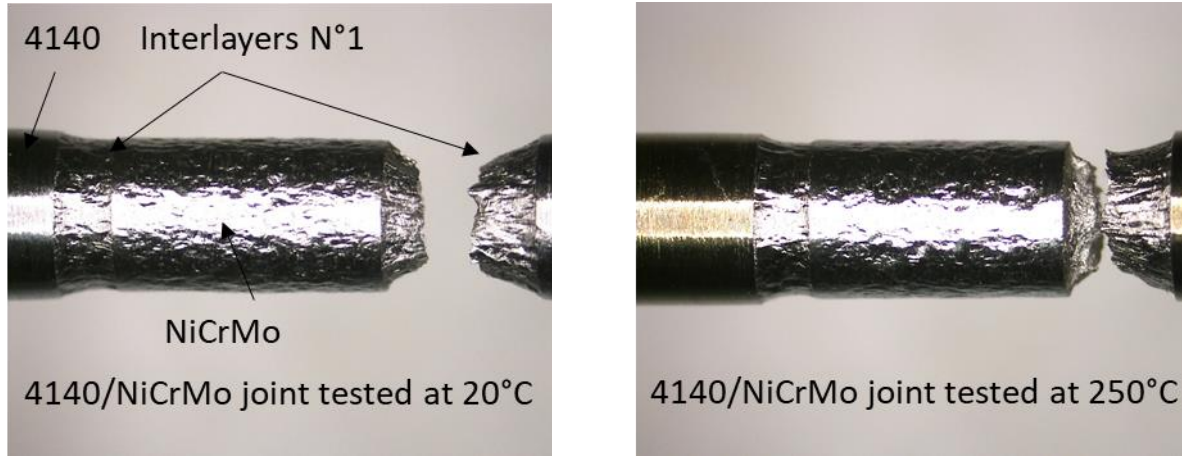


Figure 50: photographs of broken 4140/NiCrMo joint tested at 20°C and 250°C at $7 \cdot 10^{-4} \text{s}^{-1}$. The rupture of the specimens occurs inside one of the two interlayers used to join 5mm thick NiCrMo plate to the 4140 steel

Table 12: tensile properties (tensile strength TS, yield strength at 0.2% elongation YS and total elongation A) of 4140/NiCrMo/4140 joint at 20°C and 250°C at $7 \cdot 10^{-4} \text{s}^{-1}$.

T	Sample	TS	YS	A%	A% metrology	A% interlayer (thickness: 7mm)	Necking
(°C)		(MPa)	(MPa)	(%)	(%)	(%)	(%)
20	Epr01	685	365	13,4	13,4	36,9	60,5
	Epr02	687	363	14,2	13,6	46,4	66,7
250	Epr03	544	266	10,5	10,0	27,8	54,9
	Epr04	546	264	11,4	10,8	30,5	55,2

Mechanical characterization of 4140/FeNiCo joint

Figure 51 shows the tensile stress-strain curves associated to the 4140/FeNiCo joints manufactured by HIP at 1100°C and 1160°C with the same 1mm thick interlayer (interlayer N°2). At 20°C, a clear difference exists between the joints HIPed at 1100°C and 1160°C. At 1160°C, the tensile specimens break suddenly at the FeNiCo/Interlayer interface with a small necking of the soft interlayer (see Figure 52). At 1100°C, the rupture of the specimens occurs inside the interlayer after a significant elongation (see Figure 52). These observations show that the 4140/FeNiCo joint manufactured by HIP at 1100°C has better tensile properties than the 4140/FeNiCo joint made at 1160°C. They show also that the joints made at 1100°C are stronger than the interlayer that remains the weakest point of the assembly. At 250°C, all the specimens break inside the interlayer whatever the HIP joining temperature (see Figure 52) which is a good point from an assembly point of view.

D2.9 Report on the development of materials and coatings Version:

Date:

25 January 2023

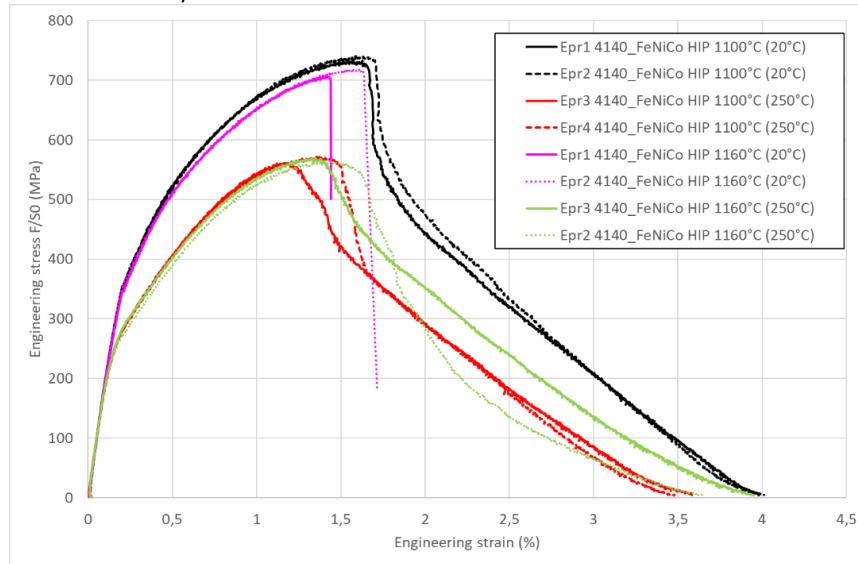


Figure 51: tensile stress-strain curves associated to the 4140/FeNiCo joints manufactured at 1100°C and 1160°C with 1mm thick interlayer N°2. Stress-strain curves recorded at 20°C and 250°C at $7 \cdot 10^{-4} s^{-1}$.

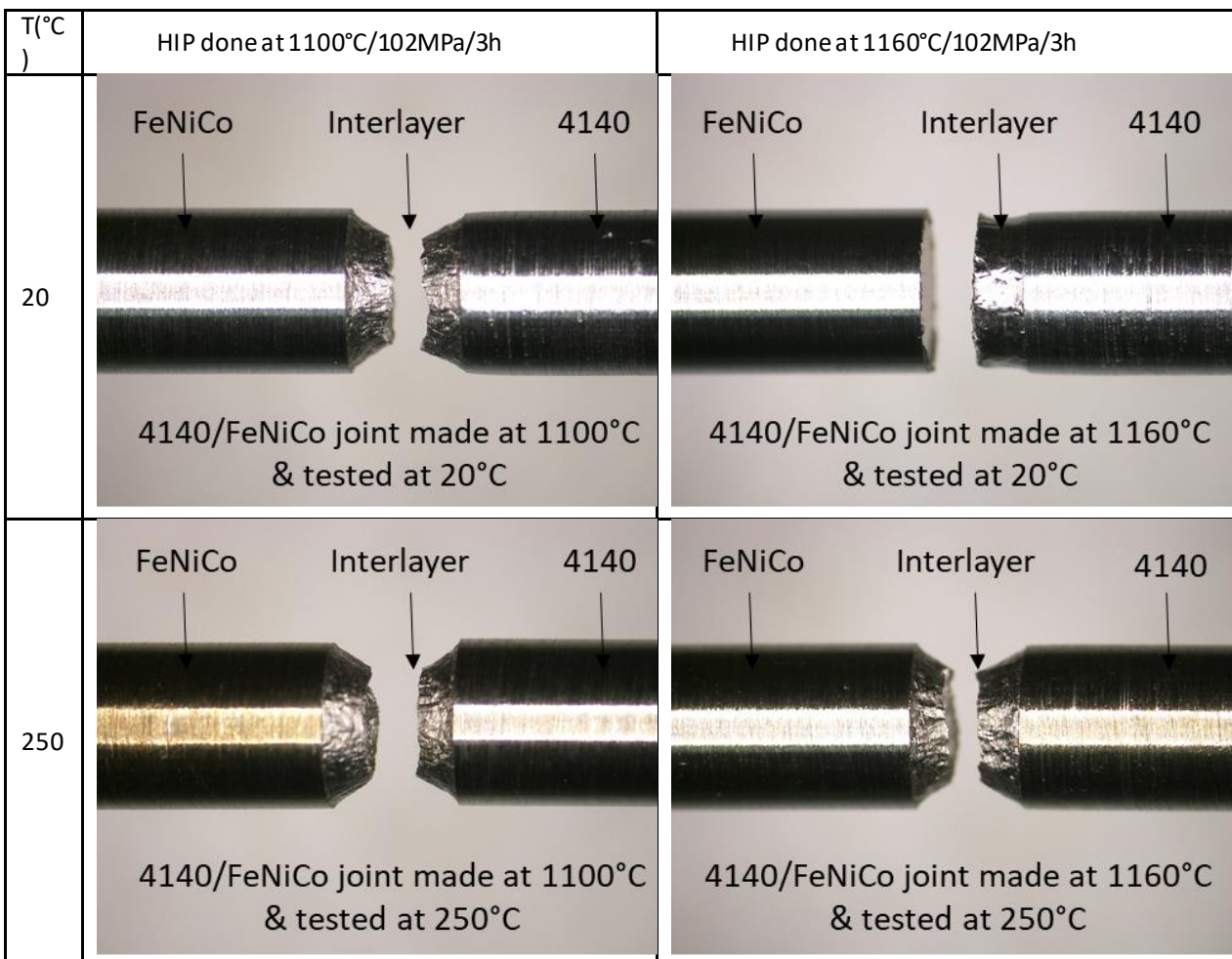


Figure 52: photographs of broken 4140/FeNiCo joints manufactured by HIP at 1100°C and 1160°C and tested at 20°C and 250°C at $7 \cdot 10^{-4} s^{-1}$.

D2.9 Report on the development of materials and coatingsVersion:

Date: 25 January 2023

The tensile tests show also that the total elongation of the specimens is small with no plasticization of the 4140 nor the FeNiCo part. The soft interlayer supports all the elongation of the specimens and metrological measurements made after the tests indicate that its deformation is about 80% at 20°C when the diffusion bonding is performed at 1100°C (only 15% when it is done at 1160°C). These measurements are tabulated in the Table 13 where we have also indicated the yield strength and the tensile strength of the tested specimens. For HIP made at 1100°C, The yield strength measured with the MTS extensometer is about 550MPa at 20°C and 350MPa at 250°C. These values are about 70% and 50% of the yield strength of the 4140 steel.

Table 13: tensile properties at 20°C and 250°C (tensile strength (TS), yield strength (YS) at 0.2% elongation and total elongation A) of 4140/FeNiCo joints made by HIP at 1100°C and 1160°C at a strain rate equal to $7 \cdot 10^{-4} s^{-1}$.

T	Sample	Manufacturing conditions	TS	YS	A	A metrology	A interlayer metrology	Necking
(°C)			(MPa)	(MPa)	(%)	(%)	(%)	(%)
20	Epr01	HIP 1100°C	735	552	3,6	4,2	87,9	54,1
	Epr02		741	550	3,7	4,1	89,1	54,8
	Epr01	HIP 1160°C	709	530	1,0	0,8	16,7	11,3
	Epr02		719	530	1,5	2,1	34,0	15,3
250	Epr03	HIP 1100°C	563	363	3,5	4,0	85,5	56,3
	Epr04		572	367	3,5	4,1	77,5	56,5
	Epr03	HIP 1160°C	570	367	3,8	4,2	93,4	56,6
	Epr04		566	348	3,8	3,5	75,1	47,5

KV impact toughness tests are machined from the 4140/Interlayer N°2/FeNiCo joints manufactured by HIP at 1100°C and 1160°C. The size of the specimens was 55x10x10mm and the V notch was located at the middle of the 1mm thick interlayer. After a metrological examination of the machined specimens, they were broken at 20°C and 250°C. The results of these tests are given in the Table 14. With an impact toughness of about 14J at 20°C and only 26J at 250°C, our experimental results show that the joints break easily at approximately the same impact energy. The rupture occurs at the interlayer/FeNiCo interface at 20°C (see Figure 53). At 250°C, the rupture occurs inside the interlayer when the joint is manufactured at 1100°C and simultaneously at the interlayer/FeNiCo interface and inside the interlayers (see Figure 53). These results confirm that the diffusion bonding of the FeNiCo high strength alloy on the 4140 steel is unsatisfactory even after the reduction of the HIP temperature.

Table 14: mean impact toughness of 4140/Interlayer N²/FeNiCo joints manufactured at 1100°C/102MPa/3h and 1160°C/102MPa/3h then oil quench from 870°C and tempered at 550°C for 2h

Mean impact toughness (J)	20°C	250°C
4140/Interlayer N ² /FeNiCo at 1100°C/102MPa/3h	14	26
4140/Interlayer N ² /FeNiCo at 1160°C/102MPa/3h	12	26



Figure 53: photographs of broken KV impact toughness specimens machined inside the 4140/interlayer N²/FeNiCo joints manufactured by HIP at 1100°C and 1160°C and tested at 20°C and 250°C.

Conclusion

Direct HIP joining of 4140 steel to a FeNiCo alloy or a NiCrMo alloy at 1160°C/102MPa/3h leads to a strong carburization of both high strength alloys. This carburization is highly visible on the metallographic samples with a decoration of the interfaces and the grain boundaries by carbides.

D2.9 Report on the development of materials and coatingsVersion:

Date: 25 January 2023

These carbides leads to an increase of the high strength alloy hardness close to the interfaces but, they also significantly reduce the mechanical strength of the joint.

To reduce their carburization, we used anti diffusion interlayers with different thicknesses. These interlayers are metallurgically compatible with both high strength alloys and have a high nickel content to avoid their own carburization during the HIP cycle. However, their mechanical properties are much lower than the mechanical properties of the materials that we want to joint by HIP. This is the main drawback of this technique and we limited their thickness to 1mm to avoid a sharp reduction of the joint's mechanical strength.

The increase of the interlayer thickness from 0.25mm to 1mm enables to reduce totally the carburization of the NiCrMo alloy. However, after an oil quench from 870°C and a tempering heat treatment done at 550°C for 2h, the hardness of the NiCrMo alloy (180HV30) is much smaller than the hardness of the 4140 steel (340HV30). Thus, this material is not suitable to reinforce the pin and the box shoulder of the tool joint. Despite this experimental result, the rupture of the joint made at 1160°C/102MPa/3h occurs always inside the interlayer with a significant elongation of the NiCrMo alloy and the soft interlayers.

At the opposite, the FeNiCo alloy has a much higher Vickers hardness (507HV30) than the 4140 steel after the post HIP heat treatments. It is thus a very good candidate to reinforce the tool joint. However, its joining to the 4140 steel is difficult and the use of 1mm thick interlayers with two different nickel contents does not allow to block totally the diffusion of carbon across the interface. Tensile tests performed at 20°C on 4140/Interlayer/FeNiCo joint made at 1160°C/102MPa/3h show that the rupture occurs at around 700MPa and always at the FeNiCo/Interlayer interface without a strong necking of the interlayer. At 250°C, the mechanical properties of the interlayer decrease leading to a rupture inside the interlayer at about 500MPa.

By keeping the same 1mm thick interlayer and by reducing the HIP temperature down to 1100°C, the carburization of the FeNiCo alloy is lower but not totally avoided. Tensile tests performed on this joint show the benefit of reducing the HIP temperature: the yield strength and the tensile strength of the joint is improved (respectively 550 and 740MPa) and all the tensile samples break inside the interlayer whatever the testing temperature (20°C or 250°C). It means that the weak point of the assembly is now the interlayer and not the interface. However, the total elongation of the specimens is small and only about some percent. This strain is only located inside the interlayer and the elongation associated only to the interlayer rises to 80%. Impact toughness tests performed on the 4140/Interlayer/FeNiCo joints made at 1100°C and 1160°C gives 14J at 20°C and 26J at 250°C. These values are much slower than the impact toughness of the 4140 (around 39J at 20°C and 125J at 250°C).

For the fabrication of the first tool joint prototypes that will be used to perform the make and break tests in the WP5, the reinforcement of the shoulders by a 5mm thick layer of FeNiCo can be tested. The FeNiCo layer will be bonded to the 4140 steel by performing the HIP at 1100°C/102MPa/3h by using a 1mm thick Ni rich interlayer. Then, the HIPed parts will be post heat treated by doing an oil quench after one hour at 870°C and a tempering heat treatment at 550°C for 2 hours to correctly harden the 4140 steel. For the fabrication of the stabilizer, a similar manufacturing can be done with the WC-Co inserts inside the FeNiCo alloy.

Task 2.6: Development and synthesis of sensor materials

PVI is performing the optimisation of Nano inks for sensor electrodes and polyimide substrate connection. Including testing for the effects of thermal shock, current overload and corrosion. To facilitate sensor production, PVI is synthesizing and manufacturing graphene/carbon enabled resistive inks from 30Ω/□ to 1000Ω/□ suitable for application at temperatures above 250°C for the strain gauge, temperature and encoder sensors. PVI has investigated various materials for printed

Date:

25 January 2023

Task 2.7: Development of Electroless (EL) plating for synthesis of PTFE based composite coating

Introduction

Hammer parts used in drilling operations for geothermal power plants are traditionally produced using low alloy steel, and are subjected to both wear and corrosion during their lifetime. Coatings with wear and corrosion resistance can be used on the hammer parts in order to improve their performance and lifetime, thereby reducing the operating and maintenance costs.

ENP is a chemical process wherein a Ni alloy (Ni-P, Ni-tungsten (W), Ni-boron (B), and Ni-copper (Cu)-P, etc) can be deposited on a metallic substrate using an aqueous solution, without the application of electric current. Properties of ENP coatings, such as their resistance to wear and corrosion, antifouling, or anti-scaling (or their combination such as corrosion resistance and anti-scaling) can further be tuned by varying the solution chemistry and/or plating processing conditions for the specific application. A reducing agent such as sodium hypophosphite is usually needed to liberate Ni ions in solution to deposit Ni metal by chemical reduction. The phosphorous (P) content of the solution, which is usually between 3 and 12%, has a strong impact on the deposited Ni properties. Therefore, industry normally identifies ENP coating according to the amount of P present in the solution e.g.:

Low P	2 – 5% P
Medium P	6 – 9% P
High P	10 – 13% P

The amount of P has a direct impact on hardness and corrosion resistance of the deposited Ni layer. Moreover, the feasibility of incorporating fine second phase particles, of submicron to nano size, within a metal/alloy matrix, has initiated a new generation of composite coatings. ENP- PTFE plating is a unique plating solution that combines the hardness of ENP with the lubricity of PTFE.

Within Task 2.7, ENP coating was developed for depositing duplex composite coating (i.e. ENP with homogeneous distribution of PTFE particles of <math><1\mu\text{m}</math>) on the low alloy steel substrates to test its suitability for the application. ENP, being a non-line-of-sight process is particularly suitable for applying coatings of thickness ranging from a few microns to tens of microns uniformly on parts with complex and intricate geometries.

The development activities within Task 2.7 included depositing duplex ENP coatings first on mild steel substrates, followed by trials on low alloy steel substrate materials. The compositions of the substrates are shown in Table 15. In order for the ENP coating to adhere to the substrate, an adhesion layer/bond coat/undercoat which contains only Ni and P was first deposited. A functional ENP layer containing a homogeneous distribution of PTFE particles (referred to as topcoat) was then deposited on top of the Ni-P undercoat. A schematic of the targeted duplex ENP coating is shown in Figure 55. P content within the deposits was targeted to be either low (2 – 5% P) or high (10 – 13% P), and therefore, the bath chemistries were set accordingly.

Date:

25 January 2023

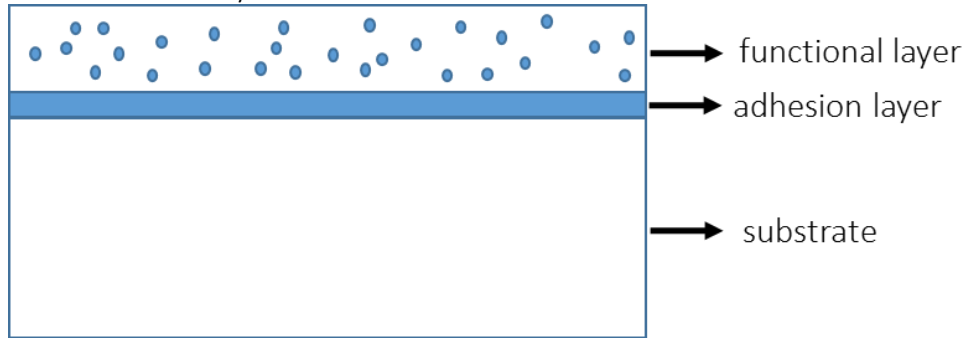


Figure 55: Schematic of duplex ENP coating. The rounded features within the functional layer represent PTFE particles.

Table 15: Nominal chemical compositions of mild steel and low alloy steel substrates

Alloy	C	Si	Mn	P	S	Mo	Cr	Ni	Ti	Cu
Mild steel	0.12	0.5	0.4	0.025	0.02	-	-	-	0.3	0.2
Low alloy steel (34CrNiMo6)	0.44	0.35	0.7	0.035	0.04	0.35	1.4	1.7	-	-

Materials and Methods

Broadly, there were five key steps involved for depositing duplex coatings onto the substrate materials (any subsequent heat treatment is considered to be a separate process):

- 1) Preparation of aqueous dispersion of PTFE particles;
- 2) Preparation of ENP bath for depositing the under coat layer onto the substrate;
- 3) Preparation of composite ENP-PTFE bath for depositing the top functional layer onto the previously deposited undercoat layer;
- 4) Preparation of the substrate surface;
- 5) Coatings deposition on the substrates.

While steps 1, 2, 3, and 5 are common for plating on mild steel and low alloy steel substrates, step 4 (substrate surface preparation) was different for two different steel types used during this work. The processing steps involved are as follows:

1) Preparation of aqueous dispersion of PTFE particles

In order to produce ENP composite coatings with a homogeneous dispersion of PTFE particles for the top functional layer, an aqueous dispersion of PTFE particles was prepared. This dispersion was then mixed with ENP bath which was used to deposit the top coat. The amount of PTFE in the top coat solution was fixed at 10g/l which was found to be suitable during another research project. PTFE particles, due to their hydrophobic nature, cannot be dispersed homogeneously in water. Therefore, a procedure was developed, which resulted in an agglomerate-free aqueous PTFE dispersion. A surfactant was used to enhance the wettability of PTFE particles by making their surfaces hydrophilic so that they can be dispersed in water. PTFE particles, along with the surfactant, were first mixed in deionised water for ~3 hours by mechanical agitation. As this mixture still contained PTFE particle agglomerates, it was followed by ultrasonic treatment for 1-2 hours. This procedure resulted in an

D2.9 Report on the development of materials and coatingsVersion:

Date: 25 January 2023

aqueous PTFE dispersion that was almost free from agglomerates. Finally, the prepared solution was further filtered via filter paper to remove leftover agglomerates or any foreign contaminants.

2) Preparation of EN bath: Undercoat

A typical ENP bath comprises a Ni ion source, reducing agent, complexing agent, accelerator, a pH regulator and a stabiliser. The key chemicals and their typical quantities used in formulating the ENP bath compositions along with the pH range used in this work are shown in Table 16. The chemicals needed for ENP were purchased from Sigma Aldrich and Fisher Scientific. The bath compositions were further adjusted for producing two different ENP coating types:

- a. low P deposits;
- b. high P deposits

Table 16: Key chemicals and their quantity (per litre) used for preparing ENP baths

Chemical	Range
Nickel sulfate	0.1-0.11M
Sodium hypophosphite	0.19-0.28M
Sodium citrate	0.035M
Acetic acid/ammonium hydroxide	Regulating pH (6.1-6.2)

3) Preparation of ENP bath: Topcoat

For depositing functional composite PTFE coating (i.e. topcoat) on the undercoat, the aqueous PTFE dispersion was mixed with the two plating solutions (low P and high P). It was ensured that plating baths contained 10g of PTFE in 1 litre of plating solution.

4) Preparation of substrate surface

The substrate surface preparation was one of the crucial steps for the production of defect-free coatings and to avoid any adhesion issue of ENP coating with the steel substrates. As mentioned earlier, initial plating trials were performed on mild steel specimens, followed by coating deposition trials on low alloy steel specimens. As the microstructure of the low alloy steel is tempered martensite, with cementite and other carbide precipitates, the substrate surface preparation method adopted was different compared with the procedure fixed for mild steel, which has a simpler microstructure (i.e. predominantly ferrite grains).

Procedures for preparing the specimen surfaces (for mild steel and low alloy steel) were developed that resulted in a Ni-P layer that adhered well with a continuous layer on the substrate surface, with no apparent macroscopic defects observed. For mild steel, the lightly oiled specimens were first dipped in a hot (~50°C) alkaline solution (10v% of aqueous solution of Decon 90™) for 15 min. They were then rinsed with running water to remove the alkaline cleaner, followed by dipping in deionised water. They were etched by transferring into a bath containing 10v.% sulphuric acid (H₂SO₄) solution in order to remove any oxide scale or corrosion products. Whereas, for low alloy steel specimens, a pre-grinding step using 1200 grit silicon carbide (SiC) paper (before dipping in alkaline solution) was found to be necessary for good adhesion of the undercoat. After grinding, the specimens were thoroughly cleaned to remove any traces of SiC particles on the substrate surface. The ground low

D2.9 Report on the development of materials and coatingsVersion:

Date: 25 January 2023

alloy steel specimens were then dipped in hot alkaline solution, followed by rinsing in deionised water and etching in sulphuric acid, following the procedure described earlier.

The time for etching depends on the thickness of oxide layer present on the sample surface. This was checked by removing the samples periodically and rinsing with water. A continuous film of water on the surface of the sample after etching was an indication that the surface was ready for ENP coating. The etched samples were then dipped in deionised water to remove any acid traces before loading into the undercoat ENP bath.

5) Deposition of ENP coatings on steel substrates

All ENP trials were performed in a fume hood with the extraction turned on. COSHH and risk assessments for all the individual chemicals were completed before preparing the solutions or performing any coating trials. Since the objective of Task 2.7 was to produce duplex coatings with Ni-P undercoat and Ni-P-PTFE topcoat on mild/low alloy steel substrates (see Figure 55 for the schematic), two baths, one with ENP solution (for undercoat) and the other with ENP+PTFE dispersion (for topcoat), were heated simultaneously on a multi-hot plate kit (Figure 56). The temperature for plating was $\sim 90^{\circ}\text{C}$. Care was taken not to overheat the plating solution as that resulted in the decomposition of the plating baths.

In order to produce specimens with duplex coatings, the cleaned and etched specimens were first immersed in the ENP bath to deposit a Ni-P layer (undercoat). After $\sim 30\text{min}$ (to achieve a targeted thickness of $5 \pm 1\mu\text{m}$), the specimens were quickly transferred into the second bath consisting of topcoat ENP+PTFE plating solution. The top functional coating deposition time range was explored in order to achieve the targeted thickness of $15 \pm 1\mu\text{m}$ before taking the specimens out for subsequent cleaning and drying. During both depositions, temperature of the solutions was maintained within the specified window while the pH was maintained between 6.1 and 6.2 along with agitating the solution with a magnetic stirrer.

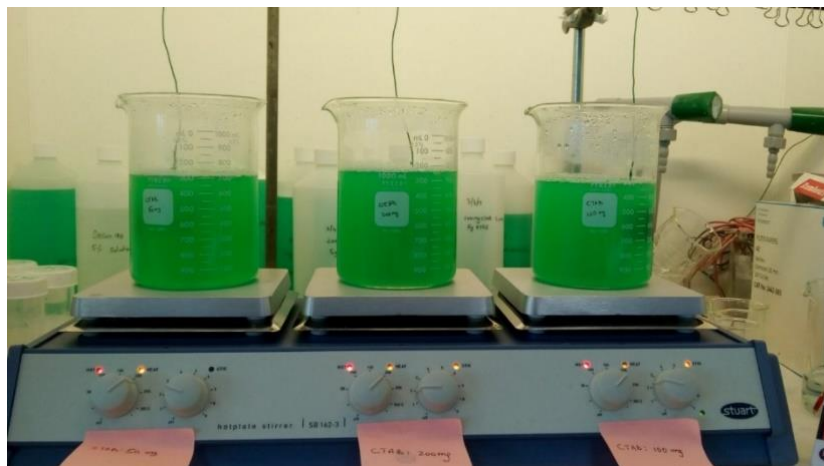


Figure 56: Multi-hotplate kit used for EN plating trials

6) Heat treatment of ENP composite coatings

As-deposited ENP coatings possess relatively low hardness, predominantly due to non-equilibrium metastable phases. These can be converted into a harder stable phase (Ni_3P α phase) after the

D2.9 Report on the development of materials and coatingsVersion:

Date: 25 January 2023

necessary heat treatment, which will enhance the coating hardness as well as wear resistance, and make the coating suitable for special applications such as hammer parts. In order to understand the effect of heat treatment on the mechanical and tribological properties of the duplex composite coatings, the following two heat treatment conditions were selected and applied using TWI vacuum electric furnace VB1 (Figure 57):

- a) 250°C for 10 hours
- b) 300°C for 2 hours



Figure 57: TWI vacuum furnace VB1

7) *Productions of ENP coatings*

Using the above coating procedure, a total of 6 coating types (Table 17) on low alloy steel substrates were produced for further characterisation and down-selection.

Table 17: Design of Experiments showing 6 different duplex ENP coating systems

Specimen identification	Undercoat	Functional topcoat	Heat treatment
HP-HP+PTFE	High P	High P + PTFE	None
HP-HP+PTFE250	High P	High P + PTFE	250°C for 10 hours
HP-HP+PTFE300	High P	High P + PTFE	300°C for 2 hours
HP-LP+PTFE	High P	Low P + PTFE	None
HP-LP+PTFE250	High P	Low P + PTFE	250°C for 10 hours
HP-LP+PTFE300	High P	Low P + PTFE	300°C for 2 hours

D2.9 Report on the development of materials and coatingsVersion:

Date: 25 January 2023

8) Characterisation of coatings

Microstructural characterisation of the ENP coated samples was performed using optical imaging and electron microscopy using field emission gun scanning electron microscope (FEG SEM). The coated specimens were sectioned and mounted in conductive Bakelite. The mounted samples were ground and polished to ¼ micron using standard metallographic procedures. SEM imaging was performed in backscattered and secondary electron modes. Surface contact angle measurements were performed using a Kruss Drop Shape Analysis system (DSA 100). Cross-cut tests were performed at RINA as per ISO 2409 standard to evaluate adhesion of the coatings. Knoop hardness of the coatings and pin on disk wear testing under dry conditions were performed for an initial down-selection of the ENP coatings at University of Iceland (UoI). Further tribological tests on the down-selected coating types were performed in 80°C water. Here, only a summary of the results are presented. Detailed analysis of the results will be provided in WP3 deliverable reports.

Duplex composite coatings on mild steel substrates

As the microstructure of low alloy steels (used for hammer parts) is tempered martensite, which is far more complex than that of mild steel (ferrite grains), initial developmental trials were carried out on mild steel specimens. These included optimisation of bath compositions, the procedures, and plating conditions (pH and temperature). The trials were performed on 25mm x 25mm x 3mm specimens. The plating trials went through several iterations, where many parameters were adjusted (chemicals used in the bath, pH and temperature) in order to produce good quality coatings (low P and high P). Finally, a procedure was developed that produced high quality duplex coatings. A representative backscattered electron (BSE) image of the cross-section of the duplex coating is shown here in Figure 58. It was seen that the coating had no macroscopic defects, with the undercoat having good adhesion with the substrate and the topcoat containing a homogeneous dispersion of PTFE particles (seen as dark features in the topcoat). With the plating procedure developed on mild steel substrates, it was then used for producing coatings on low alloy steel specimens.

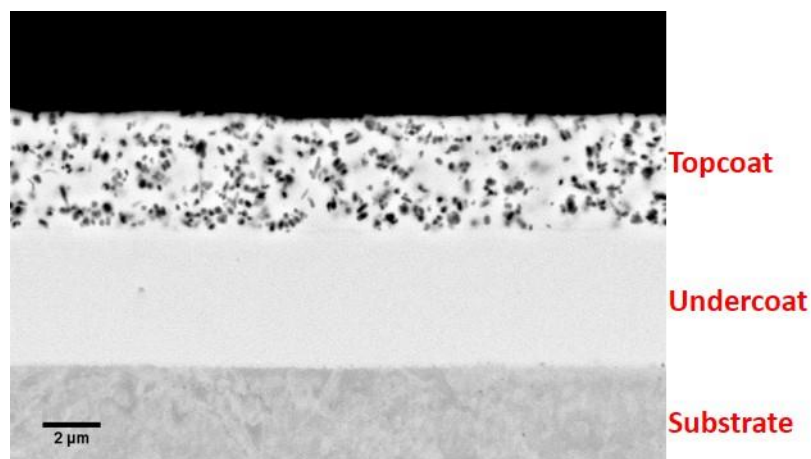


Figure 58: Backscattered electron (BSE) micrograph showing undercoat and topcoat with PTFE particles on mild steel specimen

Duplex ENP composite coatings on low alloy steel substrates

Although the procedure developed for depositing duplex composite coatings produced excellent coatings on mild steel specimens, the coatings on low alloy steel were found to contain defects. Representative optical images showing the results from initial trials on low alloy steel specimens are

D2.9 Report on the development of materials and coatingsVersion:

Date: 25 January 2023

shown in Figure 5a and Figure 59b. The etching procedure followed for mild steel substrates was used for low alloy steel specimens, however it did not result in continuous coating, with the quality of coating being very poor (Figure 5a). On slightly increasing the etching temperature and time, there was some deposition observed, although it did not result in a well-adhered coating (Figure 59b). Therefore, attention was focused towards developing a suitable surface preparation method for low alloy steels. After several attempts, it was found that grinding/polishing with SiC and cleaning the surface prior to hot alkaline cleaning followed by etching resulted in well-adhered coatings.

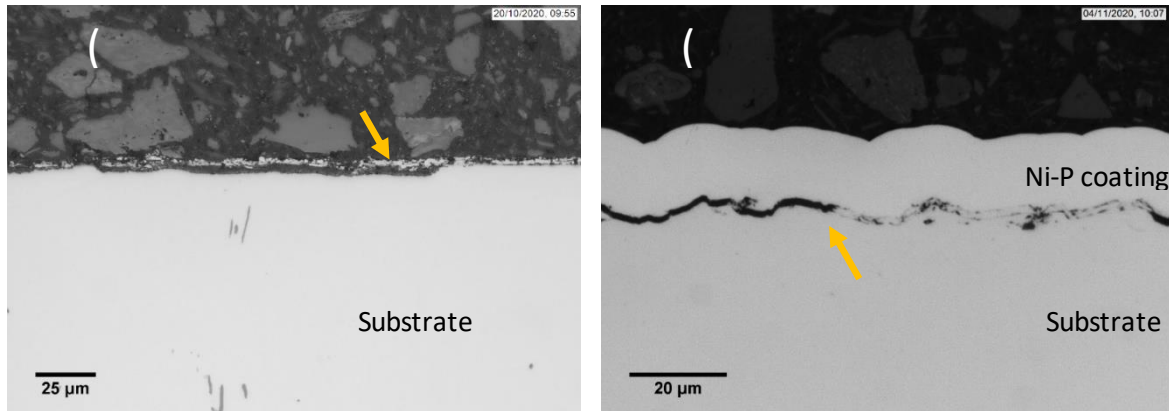


Figure 59: Optical images of the cross-sections of coatings on low alloy steel specimens: (a) After mild steel etching procedure; the arrow points to discontinuous coating; (b) After longer etch at higher temperature; coating not adhered completely to the surface

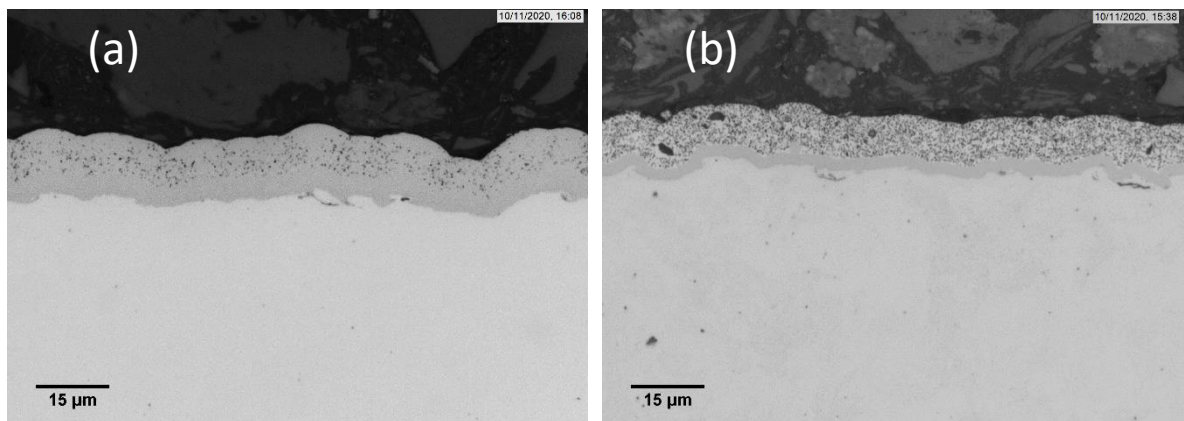


Figure 60: Optical images of the cross-sections of coatings on low alloy steel specimens: (a) High P undercoat + high P-PTFE topcoat; (b) High P undercoat + low P-PTFE topcoat

Representative optical images of the cross-sections of the coatings on low alloy steels with the improved substrate surface preparation method are shown in Figure 60a and Figure 60b. It was seen that a well-adhered coating was obtained for the two coating types, i.e. high P undercoat + high P-PTFE topcoat (Figure 60a) and high P undercoat + low P-PTFE topcoat (Figure 60b). SEM images of cross-sections of high P undercoat + high P-PTFE topcoat in the as-plated and heat treated conditions are shown in Figure 61a, Figure 61b (250°C, 10 hours), and Figure 61c (300°C, 2 hours), respectively. No apparent defects were observed in the coatings after the heat treatments. SEM images of cross-sections of high P undercoat + low P-PTFE topcoat in the as-plated and heat treated conditions are shown in Figure 62a, Figure 62b (250°C, 10 hours), and Figure 62c (300°C, 2 hours), respectively. In these coatings as well, no apparent defects were observed after performing the two different heat treatments.

D2.9 Report on the development of materials and coatingsVersion:

Date: 25 January 2023

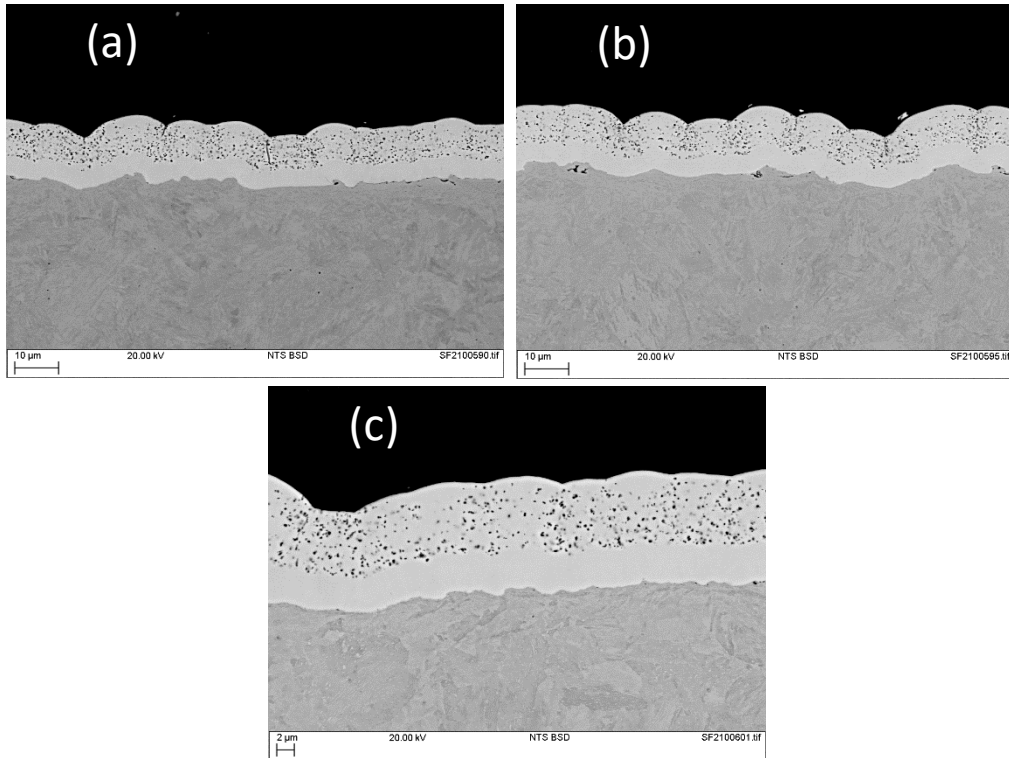


Figure 61: BSE images of the cross-sections of high P undercoat + high P-PTFE topcoat coatings on low alloy steel specimens: (a) As-plated; (b) Heat treated at 250°C for 10 hours; (c) Heat treated at 300°C for 2 hours

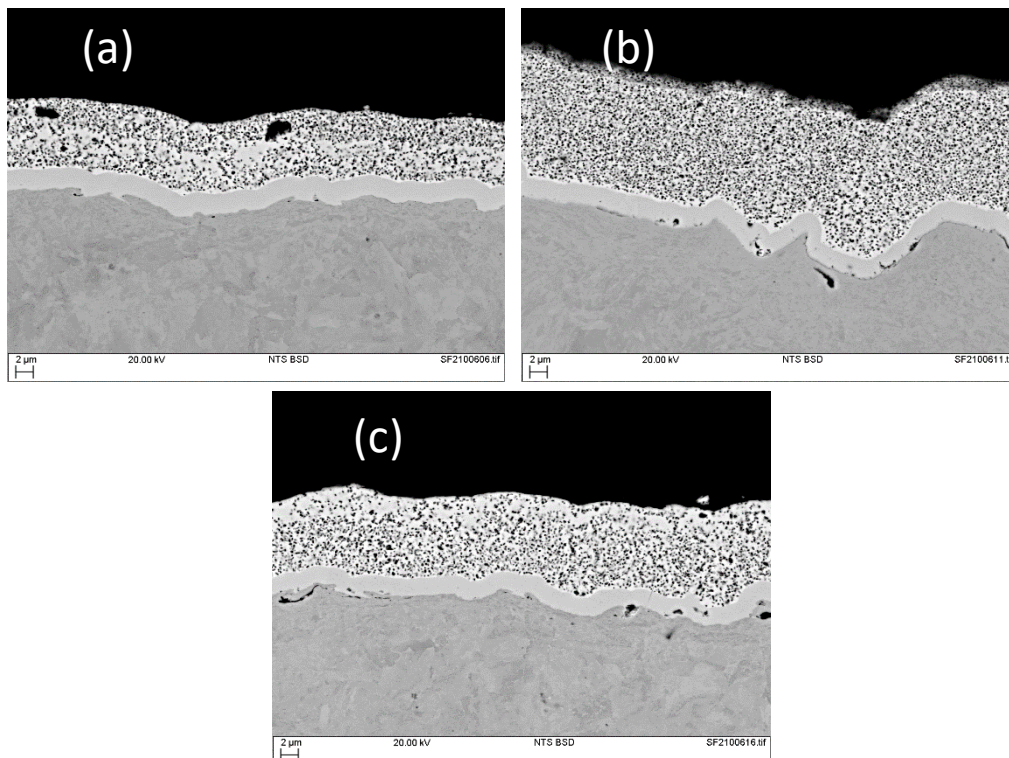


Figure 62: BSE images of the cross-sections of high P undercoat + low P-PTFE topcoat coatings on low alloy steel specimens: (a) As-plated; (b) Heat treated at 250°C for 10 hours; (c) Heat treated at 300°C for 2 hours

D2.9 Report on the development of materials and coatingsVersion:

Date: 25 January 2023

Characterisation of ENP coated Specimens

Cross-hatch tests were performed on all 6 coated specimens (see Table 17) in order to evaluate their adhesion onto the low alloy steel substrates. This test complemented the microstructural examination of the cross-sections of the coatings (Figure 61 and Figure 62). A representative photograph of the tested specimen is shown in Figure 63. All coatings had excellent adhesion with the low alloy steel substrate, and the coatings were classified as “Grade 0”, which represents a very good adhesion of the coating to the substrate as per ISO 2409 standard.

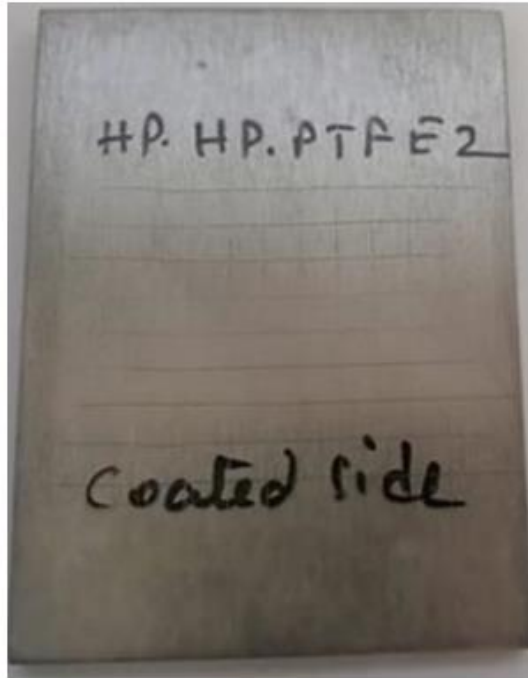


Figure 63: A representative photograph of the coating with cross-hatch markings on the surface

Contact angle measurements, coefficient of friction, track width, and Knoop hardness of the coatings are summarised in Table 4. It was seen that, compared with other coating systems, high P undercoat with low P + PTFE topcoat coating heat treated at 300°C for 2 hours (specimen ID as per table 4: HP-LP+PTFE300) had very low coefficient of friction and track width, in addition to having high hardness. The tribological testing was performed under dry conditions. Additional tribological testing under 80°C water was performed on two heat treated specimens i.e, HP-HP+PTFE300 and HP-LP+PTFE300. The coefficient of friction was measured to be around 0.27 ± 0.07 and 0.33 ± 0.09 , respectively. Comparing the values with dry friction for the two coating types (0.66 ± 0.03 and 0.24 ± 0.05 , respectively; Table 18), it was seen that the value decreased for HP-HP+PTFE300 while it increased for HP-LP+PTFE300, although the change was much higher for HP-HP+PTFE300 (60% drop) compared with HP-LP+PTFE300 (27% rise). Since both dry and wet conditions will be encountered during drilling, HP-LP+PTFE300 coating was down-selected as it had better properties compared with other coating types. This coating will be deposited on low alloy steel specimens for high pressure-high temperature corrosion, tribo-corrosion, and erosion-corrosion tests as part of WP3 (a total of 25 specimens, Figure 64).

Table 18: Summary of the test results

Specimen	Water contact angle [°]	Coefficient of Friction	Track width [mm]	Knoop hardness [HK0.05]
Substrate	68±0.34	0.51±0.09	1.22±0.09	372.4±20.6
HP-HP+PTFE	99.4±2.1	0.76±0.11	1.34±0.01	402.5±60.9
HP-HP+PTFE250	101.6±5.8	0.69±0.14	0.86±0.01	48.4±49.5
HP-HP+PTFE300	94.5±1.5	0.66±0.03	0.42±0.03	474.1±87.8
HP-LP+PTFE	99.3±5.3	0.22±0.03	0.4±0.06	236±44.4
HP-LP+PTFE250	99.7±0.8	0.26±0.07	0.32±0.05	273±43.7
HP-LP+PTFE300	91.6±0.3	0.24±0.05	0.25±0.07	393±70.4



Figure 64: Photograph showing all the ENP specimens that were produced for testing in WP3

Conclusions

Within Task 2.7, ENP duplex composite coatings were developed on low alloy steel substrates. Initial trials were focused on developing the process on mild steel substrates, followed by the trials on low

D2.9 Report on the development of materials and coatingsVersion:

Date: 25 January 2023

alloy steel specimens. Several trials were performed on low alloy steel specimens in order to produce high quality duplex coatings with high P undercoat, and low P and high P functional topcoats with embedded PTFE particles on a consistent basis. Two different heat treatments i.e. 250°C for 10 hours and 300°C for 2 hours were performed on as-deposited coatings. Microstructural characterisation, PoD wear test in dry conditions and in 80°C water, cross-cut tests, contact angle measurements, and Knoop hardness tests were performed in order to down-select one coating type for producing coatings on specimens for WP3. Based on the test results, the high P undercoat with low P+PTFE top functional layer heat treated at 300°C for 2 hours was down-selected. This coating has been deposited on the following specimens (29 in total; Figure 10):

- Discs with ϕ 30mm and 3mm thick, for tribo-corrosion tests to be conducted at University of Iceland. (4 specimens).
- Plates with 50mm x 25mm x 3mm dimension, for high pressure high temperature corrosion tests to be conducted at University of Iceland. (13 specimens).
- Plates with 59.3mm x 20mm x 3mm dimensions, for Pin-On-Disk sliding tests to be conducted at RINA (2 specimens).
- Discs with ϕ 89mm and 6.5mm thick, for tribo-corrosion tests to be conducted at RINA. (2 specimens).
- Discs with ϕ 40mm and 6.5mm thick, for erosion-corrosion tests to be conducted at TWI. (8 specimens).

Testing will be performed within WP3 and the suitability of ENP coatings will be evaluated based on the test results.

Task 2.8: Development of HEA and cermet coating

Please refer to D2.8 of Geo-Drill submitted deliverables.

3. CONCLUSIONS

In this work package, a range of materials/coatings were studied and a HIP process was also explored to improve lifetime of Geo-Drill components. The conclusions drawn from this WP are:

T2.1: A blending process of WC-Co/GO (rGO) has been developed to obtain a good dispersion of GO in WC powder. Both pure WC-Co and WC-Co/GO bulk materials were prepared through sintering for further testing.

T2.2: For hammer coating development, GO was successfully mixed with Xylan at various concentrations. Coatings were prepared on steel substrates. Preliminary testing indicated that samples with extra low percentage of GO with Xylan has the best performance. For sensor coating development, powder mixtures of PTFE and GO were prepared to introduce into PVI's polymeric matrix. After parametrisation and preparation of the mixtures, PVI prepared the inks, and the screen-printed samples were sent to WP3 for further characterisation.

T2.3: Four coatings with the best overall characteristics (from the process conditions tested) from each material type were selected after parameter development using HVOF spraying, including WC-Co-Cr, CrC-NiCr, self-fluxing and Fe-based amorphous coatings. Their surface roughness ranges from 3.5 to 8.5 μ m, porosity ranges from 0.9 to 3.6%, and hardness ranges from 661 to 1218HV_{0.3}.

Date: 25 January 2023

T2.4: A HIP process was investigated to bond the WC-Co tooth onto drill bit. Results showed that direct bonding of WC-Co tooth to 4330V steel at 1160°C/102MPa/3h led to a weak interface. A joint free of cracks was obtained by applying a selected interlayer after the HIP. However, cracking of WC-Co tooth was noticed after post-treatment. This was ascribed to martensitic transition of 4330V steel which significantly influenced stress of the teeth. It is therefore proposed to stop quenching at a temperature above Ms and then to cool slowly under calm air before doing final tempering heat treatment during manufacturing process in WP5.

T2.5: The bonding of two selected high strength alloys (FeNiCo and NiCrMo) to 4140 steel were studied using HIP. HIP bonding was carried out by anti-diffusion foils to avoid carburization of both alloys. Post heat treatments were performed on the manufactured joints to harden the 4140 to required hardness. Tensile tests showed that the bonded joints have much lower impact toughness compared with 4140. It is proposed that wear resistance of tool joint can be improved by bonding a 5mm thick FeNiCo ring on the shoulder at 1100°C/102MPa/3h, following post heat treatments. A similar manufacturing process can be used for fabrication of stabilizer.

T2.6: A wide range of materials for use in the main components of the GeoDrill sensor string are being studied. The main issue encountered was the thermal insulation of the sensors and energy storage system. Accordingly, PVI have continued to develop means to protect the sensors and devised an alternative energy storage system for the sensor string. Testing conducted by the University of Iceland in Work Package 3 indicated good performance of the materials under 'normal' drilling conditions. They also concluded with testing to identify the extremes to which the materials could be subjected, including high pressure and heat as well as immersion in corrosive chemicals.

T2.7: An electroless nickel-phosphorus plating process for PTFE based composite coatings on low alloy steel substrates was developed. Both compositions were developed for producing both low P and high P coatings. Heat-treatments were also performed to alter the microstructure by generating crystalline phases to improve coating's mechanical and tribological properties. Results indicated that specimens with high P undercoat and low P+PTFE topcoat, heat-treated at 300°C for 2h had better performance.

T2.8: Further three coatings were synthesised using HVOF spraying, including WC-Ni, WC-CrC-Ni and high entropy alloy coatings. The optimised coatings have surface roughness ranges from 3.9 to 6.6 µm, porosity ranges from 1.6 to 2.0%, and hardness ranges from 558 to 1077HV_{0.3}.

REFERENCES

- [1] H. L. Tian, M. Q. Guo, Z. H. Wang, Z. H. Tang, Y. J. Cui, *Surf. Eng.* 2017, 34, 762
- [2] K. Kornaus, A. Gubernat, D. Zientara, P. Rutkowski, L. Stobieski, *Pol. J. Chem. Technol.* **2016**, 18, 84.
- [3] C. F. Gutierrez-Gonzalez, A. Smirnov, A. Centeno, A. Fernández, B. Alonso, V. G. Rocha, R. Torrecillas, A. Zurutuza, J. F. Bartolome, *Ceramics International* 41, 6, 2015, 7434.
- [4] G.S. Upadhyaya, "Cemented tungsten carbides: production, properties, and testing", Noyes Publications, 1998.
- [5] V. K. Sarin and al., "Comprehensive hard materials volume 1", Elsevier Publications, 2014.
- [6] <https://www.jaoilfield.com/products/hole-quality/>